IEEE Access
Multidisciplinary ⋮ Rapid Review ⋮ Open Access Journal

Received 12 April 2024, accepted 3 June 2024, date of publication 11 June 2024, date of current version 21 June 2024.

Digital Object Identifier 10.1109/ACCESS.2024.3412888

RESEARCH ARTICLE

Passivity-Based Nonlinear Control Approach for Efficient Energy Management in Fuel Cell Hybrid Electric Vehicles

MUHAMMAD KHALID, (Senior Member, IEEE)
Electrical Engineering Department, King Fahd University of Petroleum and Minerals (KFUPM), Dhahran 31261, Saudi Arabia
Interdisciplinary Research Center for Sustainable Energy Systems, KFUPM, Dhahran 31261, Saudi Arabia

e-mail: mkhalid@kfupm.edu.sa

This work was supported by the King Abdullah City for Atomic and Renewable Energy (K.A.CARE).

ABSTRACT This study investigates a hybrid system comprising a fuel cell (FC), a battery, and an ultra-capacitor (UC) that drives a car. The primary focus of the research is to integrate passivity theory into the control strategy for DC-DC power converters in fuel cell hybrid electric vehicle systems (FCHEV). A fault-tolerant control scheme, coupled with energy management, is formulated, considering the battery, FC, and UC, with specific attention given to addressing challenges related to nonlinearity and fault control robustness. The work presents the mathematical modeling of the system using a passivity-based nonlinear control approach. The manuscript outlines a method for determining reference currents for batteries, FCs, and UCs, streamlining current distribution to optimize overall system efficiency. The control framework incorporates passivity theory principles to ensure control and stability. In comparison to other advanced control methods like variable structure control and backstepping control, the proposed passivity-based nonlinear control approach demonstrates efficiency gains of 29.9% and 38.5% in settling time, respectively, particularly in the context of controllers for tracking I_{UC}^{*}. The effectiveness of the proposed approach becomes evident when examining the root mean square (RMS) voltage, where it outperforms by 49.9% and 43.4%, respectively, in terms of efficiency. The superiority of the scheme is further evident in the domain of controllers for tracking the V_0^{*} profile. In this context, the proposed approach showcases a remarkable efficiency improvement of 22.4% and 36.7% in settling time and RMS voltage, respectively. Another novel aspect of study is consideration of sensor and SOC faults. In the event of a 30% and 50% fault scenario for SOC, the initial reference current for the battery is 1.9 A and 0.8 A, respectively. The results further demonstrate that the incorporation of supplementary control input, including an energy shaping component and a fractional-order proportional-derivative sliding mode surface, enhances the controller's performance by expediting convergence and improving the closed-loop FCHEV system's robustness. The use of fault-tolerant control and the energy management system yields positive and satisfactory outcomes, as the battery compensates for the lost power of the faulty FC based on its available energy. The obtained results align precisely with the proposed scenario, contributing to the ongoing development of sustainable energy solutions and transportation.

INDEX TERMS Battery, fuel cell, ultra-capacitor, energy management, fractional-order sliding mode control, hybrid electric vehicle, passivity theory.

I. INTRODUCTION

Due to the expanding demographics and advancements in both emerging and advanced nations, the demand for energy becomes more essential [1], [2], [3]. Global efforts

The associate editor coordinating the review of this manuscript and approving it for publication was Emanuele Crisostomi.

TABLE 1. Acronyms, units and definitions.

Nomenclature			
χ, u, y	State, input and output vectors	FCHEVs	Fuel cell hybrid electric vehicle
$H(\chi)$	Semi-definite positive function	EVs	Electric vehicles
$Q \in \mathcal{R}^{n\times n}$	Positive definite diagonal matrix	FC	Fuel cell
d	Non-negative function	UC	Ultra capacitor
PBC	Passivity-based control	RBFNNs	Radial Basis Function Neural Networks
PEMFC	Proton-exchange membrane fuel cell	$V_{act}, V_{conc}, V_{ohm}$	Activation, concentration and ohmic voltage drops
I_{UC}, R_{UC}	Current and internal ressistence of ultra-capacitor	PWMS	Pulse-width modulation signals
MPC	Model predictive control	SMC	Sliding mode control

are focused on developing alternative and environmentally sustainable energy systems [4], [5], [6]. This is of great importance due to the declining supply of fossil fuels and the growing concerns about the environment [7], [8], [9], [10], [11]. In the present setting, there is a growing recognition of the significance of sustainable transportation solutions. These solutions aim to mitigate environmental pollutants and improve transportation systems [12], [13]. Electric vehicles (EVs) have emerged as a key answer. They heavily depend on electric power, especially when paired with advancements in battery science [13], [14], [15]. The incorporation of these elements has broadened the range of travel destinations and improved the accessibility of charging amenities. As a result, costs have been reduced, making it more feasible for EVs to be adopted on a larger scale. Nevertheless, there are still some challenges that persist, including the limited driving range and lengthy charging periods, which present obstacles to the widespread acceptance of electric vehicles. Thus, the most effective approach is to embrace a hybrid framework that combines different power sources and storage devices. This approach enables the utilization of the advantages of specific sources while minimizing the limitations of others. Based on the current situation, it is clear that the automotive industry is playing a major role in the shift towards fuel cell (FC) EVs. This transition entails a departure from traditional vehicles powered by fossil fuels [16]. However, a recent study has shown that fuel cells may not perform at their best when faced with sudden and substantial increases in electrical power generation [17]. Furthermore, it is important to note that FCs operate by transferring energy in one direction only, which means they cannot harness and utilize energy generated from regenerative braking. Presented in this study is a novel hybrid system that combines a FC, a battery, and an ultra-capacitor (UC) to optimize the energy efficiency of vehicles.

This study presents a novel approach to system mathematical modelling by employing the passivity-based nonlinear control methodology. The manuscript also describes a way to figure out reference currents for batteries, FCs, and UCs, which makes current allocation more efficient for the best system performance. The control framework integrates the tenets of passivity theory to guarantee control and stability. This paper introduces innovation through a smart energy management scheme that utilizes passivity theory. The goal is to determine the optimal energy distribution among sources, especially in the presence of faults affecting storage devices like the state-of-charge in batteries.

A. LITERATURE REVIEW

The integration of an UC and battery as additional storage has the potential to augment the dependability and efficiency of the fuel cell hybrid electric vehicle (FCHEV). In this context, a novel method is described for managing a microgrid that makes use of distributed electricity sources and a supercapacitor storage device for energy in [18]. The researchers developed a novel data-storage function and performed an in-depth examination. One significant drawback of the supercapacitors used is their comparatively lower energy density, thereby limiting their total energy storage capacity. To guarantee optimal planning and highly effective functioning of battery power storage networks, a bi-level optimisation framework was presented in [19]. The findings of the study reveal the most effective and efficient characteristics of energy storage systems for typical use. However, the mentioned study did not consider real-world constraints when optimizing. The synchronised dynamic passive control based on perturbation estimates has been suggested in research [20]. The suggested method can reduce the need for a detailed model of the system in the typical control setup. However, the study lacks in terms of stability criteria.

The FCs take on the primary role of supplying electricity, whereas the battery and UC function as supplementary power sources. As outlined by Panagopoulos e al. [21], the battery plays a crucial role in efficiently storing energy generated during braking, providing valuable support to the FC due to its notable energy density. However, this advantageous energy

storage capability during braking may introduce challenges such as elevated weight and complexity, stemming from the requirement for larger and heavier battery systems. Striking a balance between the benefits of enhanced energy recovery and the potential drawbacks of increased overall system weight and cost is essential for optimizing hybrid energy systems like FCHEVs.

The UCs, characterized by their impressive power density, function as an effective energy reservoir, supporting the FC in handling transient and peak load situations. Integration of DC-DC converters allows the consolidation of multiple energy sources onto a centralized DC bus. This configuration facilitates the efficient transmission of energy to motors through DC-AC inverters. Sezen et al. [22] used a finite element method to simulate a high-power switching reluctance motor that was made to work in FCHEV systems. While finite element analysis offers precision in motor design and performance assessment, its computational demands may extend design and analysis time. The researchers in the study [23] have designed a customized multi-input-multi-output DC-DC power converter explicitly for an electric propulsion system. Nevertheless, creating such a bespoke converter can result in elevated initial development costs and increased system complexity. The investigation conducted in [24] examined the influence of temperature on the operational efficiency of a fuel cell hybrid electric vehicle (FCHEV). The study revealed a positive correlation between temperature and efficiency. However, concentrating solely on temperature-related effects might overlook other factors influencing the overall efficiency of FCHEVs. In contrast, Jiang et al. [25] focused on determining the optimal dimensions for various FCHEV components to minimize energy consumption. Hence, it is crucial to implement a well-crafted control strategy and energy management framework to efficiently distribute energy among the three sources, considering the prevailing load conditions.

Diverse strategies have been proposed to tackle the energy management challenges of hybrid vehicles. In [26], the authors focus on formulating a model that captures system dynamics and subsequently develop techniques for nonlinear control. However, this work may not explicitly discuss the implementation challenges and real-world applicability of the derived model and control techniques. In [27], on the other hand, a control strategy using backstepping is suggested as a way to deal with the nonlinear nature of FCHEV systems and make sure they finally converge. While backstepping control proves effective in addressing nonlinearity, it is crucial to consider its computational overhead and practical implementation to ensure its viability in real-world FCHEV systems.

The research in [28] introduces a hierarchical energy management system to enhance fuel efficiency in hybrid electric cars utilizing a combination of battery, FC, and UC technologies. This approach improves fuel utilization, operational capabilities, and energy resource resilience. Conversely, Fathabadi [29] propose a novel pulse width modulation approach for controlling the DC bus voltage in hybrid electric vehicles, demonstrating enhanced performance in terms of maximum velocity and acceleration. However, this method does not thoroughly address potential electromagnetic interference issues associated with pulse width modulation control. Qiu et al. [30] utilize model predictive control to optimize the operational effectiveness of hybrid vehicles, focusing on velocity optimization within a specified time period. Rahman et al. [31] explore variable structure control in FCHEVs to achieve overall system stability under varying loading conditions. However, this method increases system complexity and may be challenging to implement practically. In [32], a fuzzy logic-based control methodology is proposed to efficiently distribute load power demand among the energy sources of FCHEVs, ensuring optimal power performance. The study in [33] introduces a decentralized control method for FCHEVs with the goal of optimizing power allocation and enhancing the vehicle's overall lifespan. Finally, in [34], a vector control method is used to properly distribute power among the different parts of FCHEVs, resulting in a good power distribution result. The summary of proposed work in comparison with other literature systematically outlines the advantages and disadvantages of the modeling approaches employed in various studies. It serves as a valuable tool for researchers and practitioners to assess the merits of different methodologies, highlighting the unique contributions and potential limitations of each approach. The proposed work distinguishes itself from existing literature by addressing significant gaps in the study of hybrid electric vehicles (HEVs), particularly in the modeling of composite systems. A critical analysis of the literature reveals a noticeable gap in comprehensively capturing the intricacies of hybrid electric vehicle models. Unlike previous works, our research aims to bridge this gap by developing a composite model that not only considers the integration of diverse energy sources but also meticulously accounts for system nonlinearities such as in works [18], [19]. Our proposed work also seeks to fill this gap by incorporating a holistic approach that optimizes the efficiency of the hybrid electric vehicle across various operational scenarios. By doing so, it aims to overcome the limitations observed in the existing literature [32], [33], [34], where the focus on efficiency balance is either insufficient or lacking.

This article highlights the progress of an energy management framework designed for FCHEVs. The framework uses passivity-based control (PBC) ideas and a storage function to make the nonlinear control method work well at keeping the system stable by enforcing passivity. The study by [35] emphasizes the simplicity and ease of implementation of PBC. PBC has found applications in various domains, such as hydro-turbine governor systems, as illustrated by [36]. Unmanned powered parachute aircraft also benefit from PBC, as discussed in the research by [37]. Additionally, as the authors of [3] explored, PBC plays a crucial role in stabilizing servo mechanism systems. Autonomous DC microgrids utilize PBC to improve their performance, as seen

in the paper referenced as [38]. In addition, PBC has been employed for the purpose of optimizing power output in wind turbines, as described in the study conducted by Yang et al. [39]. Furthermore, the research [40] has emphasized the advantageous impact of PBC on autonomous cars. The wide range of applications demonstrates the adaptability and efficiency of PBC in several technical fields. Despite the extensive study and implementation of PBC in many engineering systems, its application in the context of FCHEVs has received limited attention in existing research. The current energy management tactics for FCHEVs mostly rely on traditional control methods, including rule-based control and optimum control, with limited exploration of the potential advantages offered by passivity-based control techniques [41], [42]. FCHEVs, being complex systems integrating fuel cells, batteries, and potentially supercapacitors, pose significant challenges in coordinating these components for optimal energy management. To address these challenges, a fault-tolerant control strategy, coupled with energy management, is developed, considering the battery, FC and an UC. The emphasis is on addressing challenges related to nonlinearity and fault control robustness. Still, more research needs to be done on passivity-based control methods that can solve integration problems and show reliable performance in a range of operational situations [43]. Additionally, FCHEVs exhibit nonlinear dynamics, including the nonlinear voltage-current characteristics of fuel cells and batteries. But, there is a hole in the academic literature when it comes to creating passivity-based controllers that take into account the nonlinearities in FCHEVs [44]. A comparison Table 2 is provided which highlights the different aspect of control and feature comparison of passivity-based nonlinear control with other optimization-based methods such as MPC and Dynamic programming (DP).

This study adopted the passive literature depending on its pertinence to the administration of energy in FCHEVs and its suitability to nonlinear devices. Although most of the research on passivity-based control primarily examines active control systems, it has been discovered that the concepts of passivity can be successfully implemented in FCHEVs to attain optimal energy allocation. The utilization of this strategy is motivated by the intrinsic nonlinearity of the system. One significant benefit of this approach is its capacity to successfully manage unpredictability, load disruptions, and input variances. Additionally, when comparing the active as well as passive control literature, it becomes evident that passive control systems provide qualities such as simplicity, resilience, wide-range application, practicality, and flexibility. These qualities make passive control approaches appealing for FCHEVs, where real-time implementation and stability are critical considerations [45]. In this study, the control approach is implemented on the DC-DC power converters responsible for connecting the energy sources to the DC bus. The FCHEV system incorporates a storage function based on passivity theory to effectively address the inherent nonlinearities. In order to tackle the issue of PBC's vulnerability, a supplementary controller has been developed. The auxiliary controller is composed of a fractional-order proportional-derivative sliding mode surface, which effectively handles parameter sensitivity. Additionally, it incorporates an energy-shaping mechanism to guarantee stability and enhance control efficacy. The main objective of the proposed PBC approach is to ensure a seamless power supply to the load and maintain a stable DC bus voltage. Additionally, it aims to ensure that the currents for each component of the hybrid storage system adhere to their designated reference values. Finally, the reference currents for the battery, FC, and UC are determined through an energy management strategy that effectively distributes appropriate current to each of the energy sources. The major contribution of the the proposed approach is as follows:

1) The incorporation of passivity theory into the control strategy for DC-DC power converters in FCHEV systems is one of our study's most significant contributions. Although passivity theory has been utilized in a variety of control domains, its application to hybrid energy systems, particularly FCHEV systems, is relatively new. The theory of passivity offers a robust framework for dealing with nonlinearities. Its application in this specific context adds a new dimension to the existing literature.
2) This study introduces an additional controller based on a sliding mode surface with fractional-order proportional-derivative coefficients. This controller is designed to effectively regulate parameter sensitivity, a crucial aspect of real-world hybrid energy systems. Combining fractional-order control techniques with sliding mode control enhances the performance of conventional methods. This combination represents a novel control engineering approach and advances FCHEV system control strategies.
3) Another novel aspect of this study centres on the management of energy in the context of faults occurrence, while considering limitations imposed by the SOC of the battery. The flexibility and durability of the presented energy control method are evaluated by conducting simulations at two different levels, 30% and 50%, for the storage.
4) An energy-shaping mechanism is an essential addition to the auxiliary controller. This method enhances system stability and control. Energy shaping has been utilized in other control applications, but its incorporation into the FCHEV system auxiliary controller is novel and enhances the performance of hybrid energy systems.
5) The work proposes a technique for calculating battery, FC, and UC reference currents using energy management. This method is required for a hybrid energy system to properly distribute current to each energy source for optimal efficiency and balance. This method improves FCHEV energy management and control comprehension.

TABLE 2. Passivity-based nonlinear control comparison with MPC and DP.

Aspect	Passivity-Based Nonlinear Control	Optimization-Based Methods (MPC/DP)
Control Approach	A control method that employs the passivity properties of the system dynamics to achieve nonlinearity.	An optimal control strategy is used to determine the most effective measures for control by solving optimization problems.
System Models	Demands a solid grasp of the system patterns and its passivity features.	Relies on precise system frameworks for identifying the optimizations problem.
Computational Complexity	Typically, the level of computation required is low, making it well-suited for practical deployment.	May pose challenges in terms of system complexity, particularly when dealing with systems of great size or intricate optimizations problems. Implementing in real-time can pose certain challenges.
Robustness	Typically able to handle unpredictability and disruptions effectively through to its passivity-based architecture.	The durability of a system relies heavily on the accuracy of the system designs as well as the effectiveness of the optimizations algorithm employed. May benefit from further enhancement methods.
Online Adaptation	It can easily be adjusted to accommodate any modifications in the system patterns or operational requirements, even when used online.	In certain situations, it may be feasible to make adjustments, although it can be quite difficult due to the requirement of solving optimizations challenges in real-time.
Stability Guarantees	Offers assurance of stability by leveraging the system's passivity.	Stability promises can be offered based on the creation and resolution strategies of the optimizations problem, but the analysis of these ensures may be more intricate.
Control Performance	While it might fail to accomplish the highest level of control efficiency, it consistently delivers stable and adequate control.	Can achieve excellent control efficiency, subject to the formulation and the efficacy of the solution.
Implementation	Well-suited for immediate use in systems that can take advantage of passivity features.	Application can pose challenges, particularly for online optimization-based techniques and may necessitate significant computing power.

The study's findings introduce a number of significant advancements to the field of energy management for FCHEVs. Significantly, the integration of passivity theory into the control strategy employed by FCHEV's DC-DC power converters presents an innovative methodology that expands the applicability of the theory to hybrid energy systems. By addressing parameter sensitivity, the introduction of a fractional-order sliding mode controller improves the efficacy of conventional methods and advances FCHEV control strategies. Furthermore, a novel contribution to FCHEV control is made with the incorporation of an energy-shaping mechanism into the auxiliary controller, which serves to improve system stability. Additionally, the research paper introduces an innovative method for determining reference currents for energy sources, thereby enhancing the comprehensibility of FCHEV energy management and control. The amalgamation of these advancements expands the limits of energy management in FCHEVs, thereby fostering the development of sustainable electric vehicle technologies.

This paper is organized as follows: Section II-A highlights the background and mathematics related to the passivity theory. A detailed model of each component of the fuel cell hybrid electric vehicle, along with the overall system model, is presented in Section III. Section IV describes the proposed architecture of the power allocation strategy and the formulated control strategy for the DC-DC converters. The simulation result and discussion are provided in Section V. The conclusion is presented in Section VIII.

II. PRELIMINARIES

This section provides an overview of the fundamental concepts and theories that form the basis of the proposed passivity-based nonlinear control approach for efficient energy management in FCHEVs. The key concepts discussed include Passivity Theory, Noninteger Calculus, Radial Basis Function Neural Networks (RBFNNs), and the Finite-Time Stability.

A. PASSIVITY THEORY

The passivity theorem ensures that each link between two passive systems through feedback will eventually result in a passive system. This approach facilitates the development of extensive passive networked systems in a modular fashion while simultaneously providing a degree of resistance against un-modeled passive dynamics. Consider the following general form nonlinear system [39]:

$$\begin{cases} \dot{\chi} = f(\chi, u) \\ y = h(\chi) \end{cases} \tag{1}$$

In this context, χ represents a state vector belonging to the real vector space $\mathcal{R}^n$. Additionally, y and u denote the output and input vectors, respectively, both residing in the real vector

space $\mathcal{R}^l$. The total energy stored is given as [39]:

$$H(\chi) = \chi^T Q \chi \geq 0. \tag{2}$$

In this context, the function $H[\chi(t)]$ is characterized as a semi-definite positive function, and the matrix Q, which belongs to the real space $\mathcal{R}^{n\times n}$, is specified as a positive definite diagonal matrix. The stored energy function satisfy energy-balance equation described by [35] and [39]:

$$\underbrace{H[\chi(t)] - H[\chi(0)]}_{\text{stored energy}} = \underbrace{\int_0^t u^T(s)y(s)d(s)}_{\text{supplied energy}} - \underbrace{\mathbf{d}(t)}_{\text{dissipated energy}} \tag{3}$$

where, the function $\mathbf{d}$ is a nonnegative representation of dissipation effects within practical systems. These effects can arise from various sources such as friction, resistance, and other mechanisms that lead to the dissipation of energy or damping in the system. The energy-balance equation above is said to be strictly output passive if $H[\chi(t)]$ is continuously differentiable and satisfies the following inequality, considering $\zeta > 0$ [39]:

$$u^T y \geq \frac{\partial H(\chi)}{\partial \chi} f(\chi, u) + \xi y^T y \tag{4}$$

Passivity theory is a key concept within the realm of control systems theory, which serves to describe the behavior of dynamic systems by examining their energy exchange with the surrounding environment. A passive system may be defined as a system that exhibits energy consumption or release over a specific duration when exposed to a limited input signal. This notion holds significant relevance in the context of energy management scenarios, namely in the FCHEVs, where the effective consumption of energy is of utmost importance. Passivity-based nonlinear control is a potent design framework for controllers, particularly for complex nonlinear systems. However, its limitations must be taken into account. These limitations include difficulties in extending it to dynamic systems, the requirement for accurate dynamic system models, the possibility of robustness issues, and computational complexity. In this work, the parameters of the controllers are fixed (i.e., they are not self-adjusting according to load demand and uncertainties), and dynamic models of the traction motor, motor-side AC converter, and tiers have been ignored to simplify the control design. Within this particular framework, the objective of a passivity-based control strategy is to develop control techniques that guarantee stability and desired performance of the system, while also adhering to rules of energy conservation.

B. NONINTEGER CALCULUS

Noninteger calculus, sometimes referred to as fractional calculus, is an expanded branch of traditional calculus that encompasses the study of derivatives and integrals of non-integer orders. The aforementioned mathematical framework offers a more precise depiction of intricate dynamical systems characterized by memory and genetic attributes. In the realm of energy management, the utilization of noninteger calculus enables us to more accurately represent the time-varying dynamics of energy storage and conversion components. This is especially pertinent in the context of hybrid systems that demonstrate transient behaviors and changeable time constants, such as FCs and batteries.

The general definition of noninteger differentiation and integration denoted by ${}_a\mathcal{D}_t^\gamma$ is [46]:

$${}_a\mathcal{D}_t^\gamma = \begin{cases} \dfrac{d^\gamma}{dt^\gamma} & \gamma > 0 \\ 1 & \gamma = 0 \\ \displaystyle\int_a^t (d\tau)^\gamma & \gamma < 0 \end{cases} \tag{5}$$

The Riemann-Liouville definition of noninteger calculus is

$${}_a\mathcal{D}_t^\gamma = \left(\frac{d}{dt}\right)^m \frac{1}{\Gamma(m-\gamma)} \int_a^t \frac{f(\tau)}{(t-\tau)^{\gamma-m+1}} \tag{6}$$

The variable m is defined as the smallest integer greater than γ, satisfying the inequality $m - 1 < \gamma < m$. Specifically, m belongs to the set of natural numbers $\mathcal{N}$, while γ is a real number in the set $\mathcal{R}$. The function $\Gamma(\cdot)$ represents the gamma function.

III. SYSTEM DESIGN AND MODELING

Figure 1 is an illustration that provides a visual representation of the topological structure of the FCHEV, which was investigated in this work. The Boost Converter and Buck-Boost Converter play a crucial role in the power control plan of EVs, allowing for effective distribution of current according to the vehicle's needs. The Boost Converter is essential for increasing the voltage from the battery to a greater value, which is frequently required to supply electricity to the motor or other high-voltage elements in the EV. The converter can be manipulated to augment the voltage provided to the motor during speeding or other instances of high-power demand, so enabling the battery's energy to be utilized efficiently and enhancing the performance of the vehicle. Conversely, the Buck-Boost Converter is very adaptable, with the ability to increase or decrease the voltage as required. The voltage provided to the motor or other components can be regulated based on the vehicle's energy management strategy. It can increase the voltage when needed and decrease it when there is excess energy. These converters have a vital function in regulating the energy flow in an EV, guaranteeing the optimal utilization of the battery's energy and optimizing the vehicle's performance. A battery, a proton-exchange membrane fuel cell (PEMFC), a UC, a DC-DC boost converter, two bidirectional DC-DC converters, and a regulating circuit are some of the components that make up the composition. The composition's is comprised of numerous critical sections. The regulatory circuit plays a significant role in permitting effective power allocation in accordance with the set plan. t is important to note that both the fuel cell and the battery serve as primary sources of energy and are able to

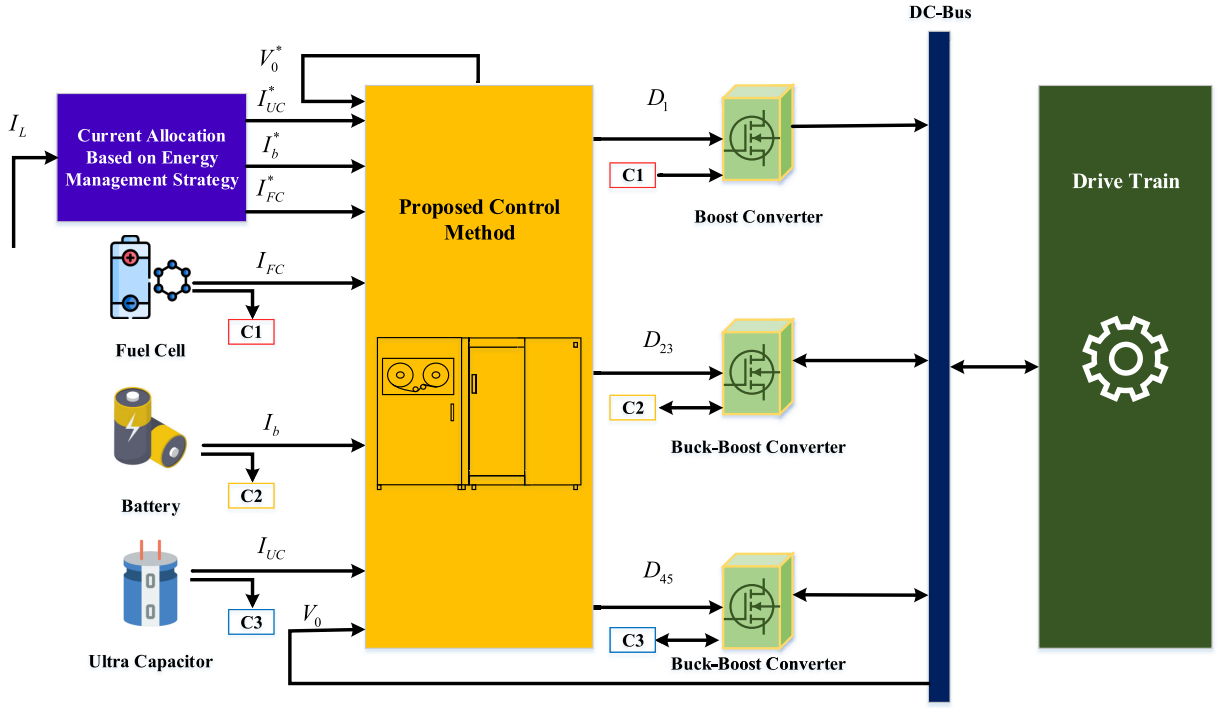

FIGURE 1. Circuit diagram of the fuel cell hybrid electric vehicle.

respond to a variety of load-power conditions. When used in conjunction with one another, the battery and the UC serve as supplementary energy storage systems, contributing to the total system in support of its operation. When the FC encounters a malfunction, operates with lower efficiency, or actively provides regenerative energy to the system, the battery smoothly occupies a central position as the major component. This occurs in situations where the FC is working with reduced efficiency.

The UC has the capability to respond to swift changes in power levels that go beyond the acceptable range for the battery and FC, thanks to its remarkable power density. There are two types of two-way DC-DC converters in fuel cell and battery systems. Each one has two insulated gate bipolar transistors (IGBTs), an inductor (called L_i when i is either UC or battery) that filters high frequencies well, and a capacitor (C_0) that does the same thing. In contrast, the boost converter is composed of a high-frequency filtering inductor (L_{FC}), an IGBT, and a diode. Both the DC-bus and the DC-AC inverters channel the resultant output currents generated by the boost converter (I_1) and the dual bidirectional converters (I_2 and I_3) into the load.

A. PEMFC MODELING

The mathematical model can be obtained using Kirchhoff's voltage law to the circuit, as follows [47]:

$$L_{FC}\frac{dI_{FC}}{dt} = V_{FC} - R_{FC}I_{FC} - (1 - D_1)V_0 \tag{7}$$

$$I_1 = (1 - D_1)I_{FC} \tag{8}$$

In this context, I_{FC} represents the current, and R_{FC} is the resistance of the PEMFC. D_1 denotes the duty cycle of the IGBT, and V_0 is the DC bus voltage. The relationship between the hydrogen consumption rate of the FC and its output current is expressed as follows:

$$m_{H_2} = \frac{M_{H_2}}{2F}I_{FC} \tag{9}$$

where m_{H_2} is the hydrogen flow rates, I_{FC} is the PEMFC output current generated from the oxidation reaction between hydrogen and oxygen, M_{H_2} is the hydrogen molar mass, and F is the Faraday constant. The PEMFC output voltage can be expressed as [28]:

$$V_{FC} = E_{FC} - V_{act} - V_{conc} - V_{ohm} \tag{10}$$

$$\begin{cases} E_{FC} = 1.044 \times 10^{-4}(T_{FC} - 298.15) + 4.385 \times 10^{-5} \\ \quad T_{FC}\, ln(P_{H_2}) \qquad + 0.5\, ln(P_{O_2}) \\ V_{act} = \iota_1 + \iota_2\, T_{FC} + \iota_3\, T_{FC}\, ln(C_{O_2}) + \iota_4\, ln(I_{FC}) \\ V_{conc} = -b\, ln\left(1 - \dfrac{I_{FC}}{I_{maxi}}\right) \\ V_{ohm} = I_{FC}\,(R_{mr} + R_{pr}) \end{cases} \tag{11}$$

where, E_{FC} is the open circuit voltage, T_{FC} is the PEMFC temperature, P_{H_2} and P_{O_2} are the partial pressures of hydrogen and oxygen, respectively, ι_i $(i = 1, 2, 3, 4)$ are parameters for the over-voltage at the electrodes, R_{mr} and R_{pr} are the PEMFC and proton resistances, respectively, V_{act} is the activation voltage drop, V_{conc} is the concentration voltage drop, V_{ohm} is the concentration voltage drop.

B. BATTERY ENERGY STORAGE MODELING

Battery energy storage systems are of great significance in contemporary energy management, particularly in the context of FCHEVs, where they assume crucial functions in the storage and provision of electrical energy. The precise representation of battery dynamics is of utmost importance in the development of efficient control methodologies aimed at maximizing energy efficiency. Within this particular section, we will explore the fundamental components of battery energy storage modeling, which encompasses the examination of both electrochemical and dynamic characteristics [48].

$$B_b = \begin{cases} 0, & \text{if } I_b^* < 0 \text{ (buck)} \\ 1, & \text{if } I_b^* > 0 \text{ (boost)} \end{cases} \tag{12}$$

$$L_b \frac{dI_b}{dt} = V_b - I_b R_b - (1 - D_2)V_0 \tag{13}$$

$$I_2 = (1 - D_2)I_b \tag{14}$$

$$L_b \frac{dI_b}{dt} = V_b - I_b R_b - D_3 V_0 \tag{15}$$

$$I_2 = D_3 I_b \tag{16}$$

$$D_{23} = [B_b(1 - D_2) + (1 - B_b)D_3] \tag{17}$$

$$L_b \frac{dI_b}{dt} = V_b - I_b R_b - D_{23} V_0 \tag{18}$$

$$V_b = V_0 - \frac{Q_b}{Q_b - \int I_b dt} + A_1 exp\left(A_2 \int I_b dt\right) \tag{19}$$

$$I_2 = D_{23} I_b \tag{20}$$

where D_{23} represents the signal of proposed control towards buck-boost converter as shown in Figure 1 during the discharging mode. To simplify the battery model and achieve a more general formulation, standardization is applied using a virtual control given by (21). Consequently, the comprehensive model of the battery, encompassing both charging and discharging, denoted by (13)-(15), is attained and expressed as:

$$D_{23} = [B_b(1 - D_2) + (1 - B_b)D_3] \tag{21}$$

$$L_b \frac{dI_b}{dt} = V_b - I_b R_b - D_{23} V_0 \tag{22}$$

$$V_b = V_0 - \frac{Q_b}{Q_b - \int I_b dt} + A_1 exp\left(A_2 \int I_b dt\right) \tag{23}$$

$$I_2 = D_{23} I_b \tag{24}$$

where V_0 is the initial voltage of the battery, Q_b is the rated capacity of the battery, A_1 and A_2 are battery constants.

C. ULTRA-CAPACITOR MODELING

The UC facilitates bidirectional current flow, enabling both charging and discharging operations. Charging of the UC is achieved through regenerative braking as well as tapping into the battery's peak power output. Consequently, a two-way converter will be employed, operating similarly to the battery's functionality. The variable denoted as B_{UC} is introduced in (25), utilizing the reference current of the UC (I_{UC}^*).

In accordance, the mathematical formulation of the converter during the UC's discharging phase (boost mode) is established in (26)-(27). This formulation involves the UC's current (I_{UC}), its internal resistance (R_{UC}), and the controlled parameter D_3. Conversely, during the charging stage, the converter's equations can be expressed as outlined in (28)-(29). The virtual control parameter is defined using the relationship given in (30).

By amalgamating the expressions from (26) and (28), the overarching equation governing the UC converter's behavior is attained, as presented in (31)-(33) [49].

$$B_{UC} = \begin{cases} 0, & \text{if } I_{UC}^* < 0 \text{ (buck)} \\ 1, & \text{if } I_{UC}^* > 0 \text{ (boost)} \end{cases} \tag{25}$$

$$L_{UC} \frac{dI_{UC}}{dt} = V_{UC} - I_{UC} R_{UC} - (1 - D_4)V_0 \tag{26}$$

$$I_3 = (1 - D_4)I_{UC} \tag{27}$$

$$L_{UC} \frac{dI_{UC}}{dt} = V_{UC} - I_{UC} R_{UC} - D_5 V_0 \tag{28}$$

$$I_3 = D_5 I_{UC} \tag{29}$$

$$D_{45} = [B_{UC}(1 - D_4) + (1 - B_{UC})D_5] \tag{30}$$

$$L_{UC} \frac{dI_{UC}}{dt} = V_{UC} - I_{UC} R_{UC} - D_{45} V_0 \tag{31}$$

$$V_{UC} = V_{UC_0}\, e^{-\left(\frac{t}{R_{UC} C_{UC}}\right)} \tag{32}$$

$$I_3 = D_{45} I_{UC} \tag{33}$$

In this context, V_{UC} and V_0 represent the voltage level and initial voltage of the UC. The amount of energy drawn from the UC, as given by (34), is determined based on the energy drawn from the UC (E_{UC}) and the capacitance of the UC (C_{UC}) [26].

$$E_{UC} = \frac{C_{UC}(V_{UC}^2 - V_{UC_0}^2)}{2} \tag{34}$$

where E_{UC} is the quantity of energy drawn from the ultra-capacitor, and C_{UC} is the capacitance of the ultra-capacitor.

D. GLOBAL SYSTEM MODELING

Global system modeling encompasses the thorough depiction and examination of intricately linked systems with diverse components and interactions. These systems encompass a wide spectrum, spanning from tangible technical systems such as power grids, transportation networks, and natural ecosystems to intangible systems within the realm of social sciences, such as economic marketplaces and information networks [50]. Applying Kirchhoff's current law, the global system of the model is developed as follows:

$$C_0 \frac{dV_0}{dt} + I_L = I_1 + I_2 + I_3 \tag{35}$$

$$C_0 \frac{dV_0}{dt} = (1 - D_1)I_{FC} + D_{23} I_b + D_{45} I_{UC} - I_L \tag{36}$$

E. ELECTRIC DRIVE TRAIN MODELING

The calculation of the power required by the electric drive system is the first step in designing an appropriate

power supply unit. This power necessity is contingent upon factors such as acceleration, the vehicle's mass, its highest achievable speed, and similar parameters. Assuming an inverter efficiency of 80%, the quantification of power needed for the electric drive system is mathematically expressed as follows:

$$P_L = \frac{1}{0.8}\left[M\frac{dv_s}{dt} + 0.5\rho_a A C_x v_s^2 + MgC_r\right]v_s \tag{37}$$

In this context, v_s represents the vehicle speed, C_r is the rolling resistance coefficient, C_x is the aerodynamic drag coefficient, g denotes the acceleration due to gravity, M is the vehicle mass, A represents the vehicle frontal surface, and ρ_a is the density of air. Assuming that the DC bus voltage remains constant throughout the operation, the current drawn by the electric drive train is calculated as shown in (38). By utilizing (7), (22), (31), and (36), the comprehensive mathematical equations governing the FCHEV are provided in (42).

$$I_L = \frac{1}{0.8V_0}\left[M\frac{dv_s}{dt} + 0.5\rho_a A C_x v_s^2 + MgC_r\right]v_s \tag{38}$$

$$\frac{dI_{FC}}{dt} = \frac{V_{FC}}{L_{FC}} - \frac{R_{FC}}{L_{FC}}I_{FC} - \frac{(1-D_1)}{L_{FC}}V_0 \tag{39}$$

$$\frac{dI_b}{dt} = \frac{E_b}{L_b} - \frac{R_b}{L_b}I_b - \frac{D_{23}}{L_b}V_0 \tag{40}$$

$$\frac{dI_{UC}}{dt} = \frac{V_{UC}}{L_{UC}} - \frac{R_{UC}}{L_{UC}}I_{UC} - \frac{D_{45}}{L_{UC}}V_0 \tag{41}$$

$$\frac{dV_0}{dt} = \frac{(1-D_1)}{C_0}I_{FC} + \frac{D_{23}}{C_0}I_b + \frac{D_{45}}{C_0}I_{UC} - \frac{1}{C_0}I_L \tag{42}$$

Based on the non-linear multi-input-multi-output (MIMO) formulation of the systems (39)-(42), it is essential to design an appropriate control method. Therefore, by controlling D_1, D_{23}, and D_{45}, the system (39)-(42) can effectively operate, and I_{FC}, I_b, I_{UC}, and V_0 can meet the load demand. Moreover, proper pulse-width modulation signals (PWMS) can be sent to the FCHEV by the controller.

F. SOC FAULT SCENARIO

The attainment of battery current balance is contingent upon the consideration of each of the SOC along with data about faults. The selection process is as follows:

$$\bar{x}_B = \left[B(e)^{\sigma t} + (1-\psi)\times I_{FC}\right]\times SOC \tag{43}$$

The Coulomb counting estimation is utilised to evaluate the SOC of the battery.

$$SOC = SOC_o - \int \frac{i_b c}{C_n}dt \tag{44}$$

The constant B is utilized to establish the starting level of the battery beginning current, whereas the constant σ is employed to determine the appropriate start-up period for the FC. The battery's state of charge is denoted by SOC, where SOC_o symbolizes the initial state of charge. The battery current is represented by $i_b c$, while C_n denotes the battery capacity. The expression representing the equilibrium progression of the battery current (referred to as expression (43)) is chosen in order to guarantee that the battery supplies the required power for the first operation of the whole thing. In the background, the FC undergoes a gradual initiation process and subsequently acquires operational control, eventually supplanting the battery. The exponential structure $B(e)^{\sigma t}$ is used to depict the interval between the end and commencement of the stack. The customization of this statement can be achieved by modifying the values assigned to variables B and σ. Significantly, the term enables a smooth and incremental shift and transfer of responsibility. The selected reference for the battery current accounts for two factors: (i) the fault condition by include a definition for the current of the malfunctioning FC, as well as (ii) the battery's cells SOC by including the SOC component. In the occurrence of a failure condition in a FC system, the decrease in power output from the FC, which is caused by the fault and quantified in relation to the current comparison, is compensated by modifications in the reference current of the battery.

The SOC of battery cells in an electric automobile plays a crucial role in determining its operational performance and efficiency. The SOC has a direct impact on the electrical power available for propulsion, which in turn has a direct influence on the vehicle's travel distance. In addition, the performance of certain models may vary as the SOC changes. This can lead to reduced energy or velocity as the SOC decreases, which is done to safeguard the battery. This study also performed three different simulations considering urban, rural, and highway driving profiles. The SOC is considered as 20% for all these simulations. In Figure 3 voltage and current profiles with respect to time for urban charging profile have been given, whereas, the voltage are reaching to maximum limit of $60V$ and current during the 20% SOC lies at $-10A$. For second phase the Figure 4 voltage and current profiles with respect to time for Rural charging profile have been given, whereas, the voltage are reaching to maximum limit of $40V$ and current during the 20% SOC lies at $-7A$. In Figure 5 voltage and current profiles with respect to time for Highway charging profile have been given, whereas, the voltage are reaching to maximum limit of $30V$ and current during the 20% SOC lies at $-5A$.

IV. ENERGY MANAGEMENT ARCHITECTURE

A. POWER ALLOCATION METHOD

The power distribution management technique may be customized based on the performance characteristics of the battery, FC, and UC. The FC intervenes by supplying the requisite electrical current in situations where there is a demand for optimal loads. Nevertheless, at periods of increased demand for power, the process of extracting current from the fuel cell is bypassed to avoid fuel shortages and undue pressure on the current, as emphasized in the cited source [26]. In such instances, the battery is utilized to ensure a continuous and uninterrupted power supply. The

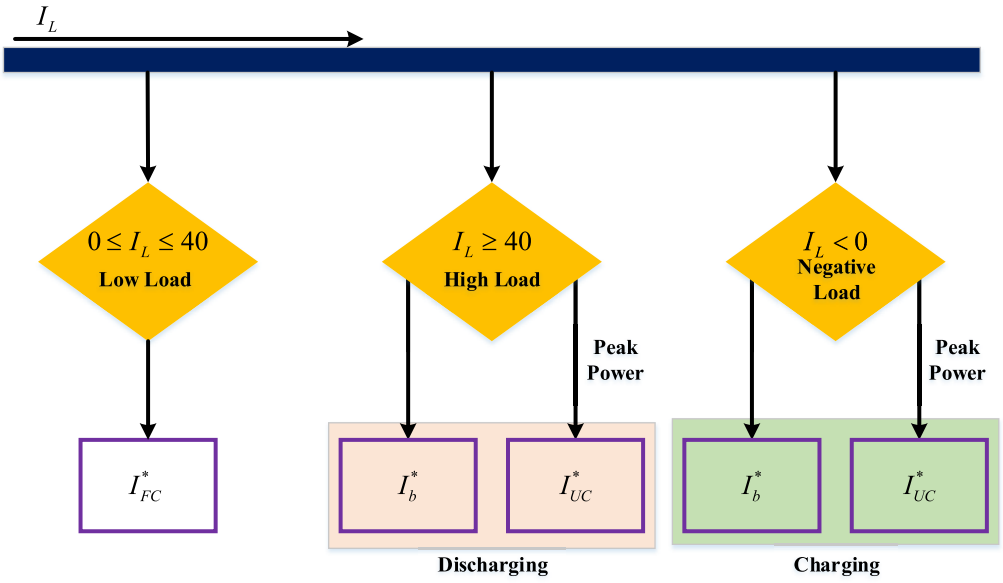

FIGURE 2. Architecture of the proposed energy management strategy.

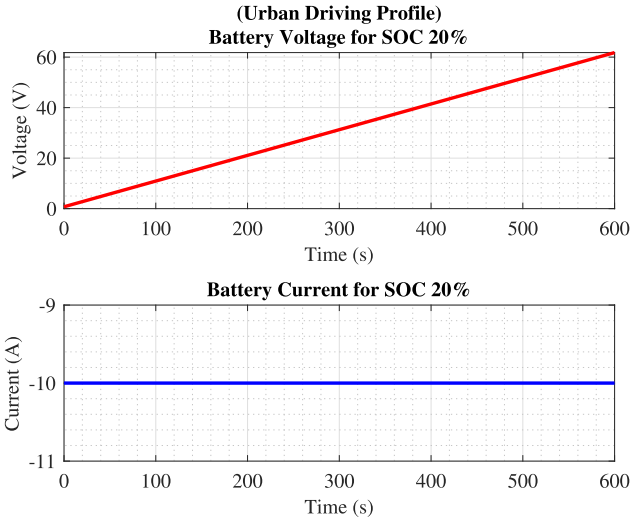

FIGURE 3. Urban charging profile impact for 20% SOC.

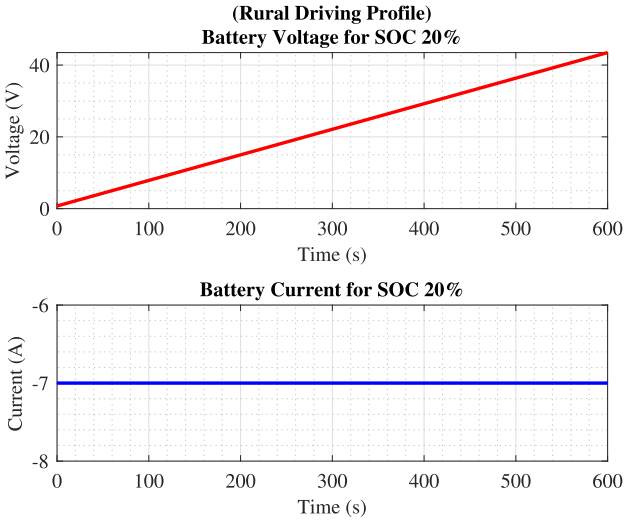

FIGURE 4. Rural charging profile impact for 20% SOC.

UC's function is to mitigate transient power fluctuations, particularly those with short-term load profile peaks that could be harmful to both the FC and battery systems. Both the battery and UC undergo charging through the recuperation of excess energy during regenerative braking, while the FC stays in a dormant state. To obtain a visual depiction of the proposed energy management approach for the FCHEV, please see Figure 2.

The following formulation results in the allocation of power:

$$P_L = P^*_{FC} + P^*_{UC} + P^*_b \tag{45}$$

In this context, the symbol P^*_b denotes the specified power reference for the battery, whereas P^*_{FC} signifies the defined power reference for the FC. Both of these power references are crucial to the power allocation approach. Moreover, the symbol P^*_{UC} represents the power allocation assigned to the UC, which is calculated based on the remaining load demand that includes energy recovered during braking and sudden increases in power demand. Hence, the determination of the reference currents for the battery, FC, and UC is achieved by assigning the load current according to the procedure described in equation (38).

1) In order to mitigate stack degradations and faults, the FC current remains positive and does not surpass a

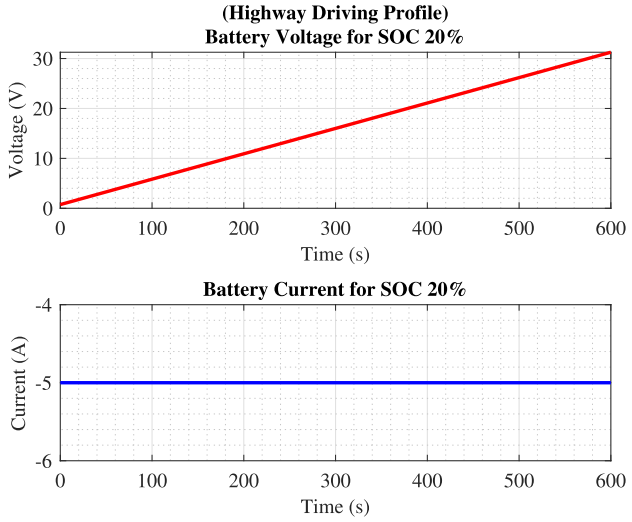

FIGURE 5. Rural charging profile impact for 20% SOC.

predetermined threshold of 40A. The reference current of the FC is calculated using a low-pass as follows [51]:

$$I_{FC}^{*} = \begin{cases} 0 & \text{if} \quad \dfrac{2\pi f_{FC}}{2\pi f_{FC}+s} I_L \le 0 \\ \dfrac{2\pi f_{FC}}{2\pi f_{FC}+s} I_L & \text{if} \quad \dfrac{2\pi f_{FC}}{2\pi f_{FC}+s} I_L > 0 \\ 40 & \text{if} \quad \dfrac{2\pi f_{FC}}{2\pi f_{FC}+s} I_L > 40 \end{cases} \tag{46}$$

where, I_{FC}^{*} is the FC reference current, f_{FC} is the low-pass filter cut-off frequency of the FC reference current.

2) Similarly, low-pass filter is utilized to calculate the reference current of the battery as follows:

$$I_b^{*} = \begin{cases} 20 & \text{if} \quad \dfrac{2\pi f_b}{2\pi f_b+s}(I_L - I_{FC}^{*}) > 20 \\ \dfrac{2\pi f_b}{2\pi f_b+s}(I_L - I_{FC}^{*}) & \text{if} \quad -20 \\ \qquad \le \dfrac{2\pi f_b}{2\pi f_b+s}(I_L - I_{FC}^{*}) \le 20 \\ -20 & \text{if} \quad \dfrac{2\pi f_b}{2\pi f_b+s}(I_L - I_{FC}^{*}) \\ \qquad < -20 \end{cases} \tag{47}$$

where I_b^{*} is the reference current and f_b is the low-pass filter cut-off frequency of the battery reference current. To extend the longevity of the battery's life cycle, a limitation is imposed to prevent its discharge from exceeding 20A or its charge from exceeding $-20A$.

3) The UC is capable of efficiently capturing high levels of power during the process of regenerative braking, and subsequently rapidly discharging power during periods of high load demand. Accordingly, the reference UC current is calculated using the following:

$$I_{UC}^{*} = I_L - I_{FC}^{*} - I_b^{*} \tag{48}$$

B. CONTROL STRATEGY

The control strategy formulated for FCHEV is shown in Figure 6. I_b, I_{FC}, I_{UC}, and V_0 are considered as control variables for ensuring and effective operation of the hybrid storage devices in accordance with the power allocation. The procedure for designing the proposed FCHEV controller is given by defining the tracking error variables z_1, z_2, z_3, and z_4 as:

$$z_1 = I_{FC} - I_{FC}^{*} \tag{49}$$
$$z_2 = I_b - I_b^{*} \tag{50}$$
$$z_3 = I_{UC} - I_{UC}^{*} \tag{51}$$
$$z_4 = V_0 - V_0^{*} \tag{52}$$

where V_0^{*} stands for the reference DC-bus voltage. Then, the relationship between the control signals and the tracking errors can be described by:

$$\dot{z}_1 = \frac{V_{FC}}{L_{FC}} - \frac{R_{FC}}{L_{FC}} I_{FC} - \frac{(1-D_1)}{L_{FC}} V_0 - \dot{I}_{FC}^{*} \tag{53}$$
$$\dot{z}_2 = \frac{E_b}{L_b} - \frac{R_b}{L_b} I_b - \frac{D_{23}}{L_b} V_0 - \dot{I}_b^{*} \tag{54}$$
$$\dot{z}_3 = \frac{V_{UC}}{L_{UC}} - \frac{R_{UC}}{L_{UC}} I_{UC} - \frac{D_{45}}{L_{UC}} V_0 - \dot{I}_{UC}^{*} \tag{55}$$
$$\dot{z}_4 = \frac{(1-D_1)}{C_0} I_{FC} + \frac{D_{23}}{C_0} I_b + \frac{D_{45}}{C_0} I_{UC} - \frac{1}{C_0} I_L - \dot{V}_0^{*} \tag{56}$$

A storage function is constructed for (54)-(56) as follows:

$$\begin{aligned} H(I_b, I_{FC}, I_{UC}, V_0) = {} & \underbrace{\frac{r_b}{2}(I_b - I_b^{*})^2}_{\text{heat by battery}} + \underbrace{\frac{r_{FC}}{2}(I_{FC} - I_{FC}^{*})^2}_{\text{heat by FC}} \\ & + \underbrace{\frac{r_{UC}}{2}(I_{UC} - I_{UC}^{*})^2}_{\text{heat by UC}} \\ & + \underbrace{\frac{1}{2r_0}(V_0 - V_0^{*})^2}_{\text{heat by DC-bus}} \end{aligned} \tag{57}$$

The stored energy function, denoted as $H(I_b, I_{FC}, I_{UC}, V_0)$, is the cumulative heat generated by the currents passing through the FC, UC, battery, and DC-bus resistors. r_b, r_{FC}, r_{UC}, and r_0 are unit virtual resistances of the battery, FC, UC, and DC-bus, respectively.

In order to account for the unknown faults $\dot{T}_1$, $\dot{T}_2$, $\dot{T}_3$, and $\dot{T}_4$, (57) is rewritten as follows:

$$H(I_b, I_{FC}, I_{UC}, V_0) = \frac{1}{2}z_1^2 + \frac{1}{2}z_2^2 + \frac{1}{2}z_3^2 + \frac{1}{2}z_4^2$$

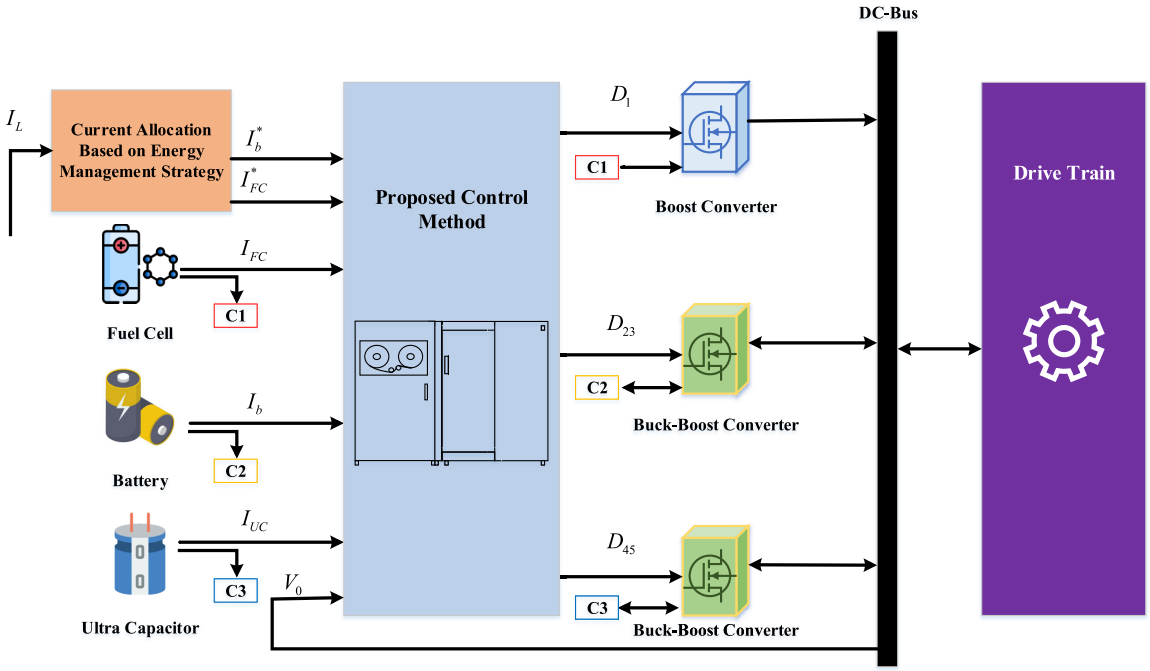

FIGURE 6. Control structure of the FCHEV.

$$+\frac{1}{2\gamma_1}\tilde{W}_1^T\tilde{W}_1+\frac{1}{2\gamma_2}\tilde{W}_2^T\tilde{W}_2 +\frac{1}{2\gamma_3}\tilde{W}_3^T\tilde{W}_3+\frac{1}{2\gamma_4}\tilde{W}_4^T\tilde{W}_4 \quad (58)$$

where $\gamma_i > 0$ $(i = 1, 2, 3, 4)$ is a design parameter, $\tilde{W}_i = W_i - \hat{W}_i$ $(i = 1, 2, 3, 4)$ is the weight estimation error, with $\hat{W}_i$ being the estimate of W_i.

The time derivative of the energy function (59) is

$$\begin{aligned}&\dot{H}(I_b, I_{FC}, I_{UC}, V_0)\\ &= z_1\dot{z}_1 + z_2\dot{z}_2 + z_3\dot{z}_3 + z_4\dot{z}_4\\ &\quad -\frac{1}{\gamma_1}\dot{\hat{W}}_1^T\hat{W}_1 - \frac{1}{\gamma_2}\dot{\hat{W}}_2^T\hat{W}_2\\ &\quad -\frac{1}{\gamma_3}\dot{\hat{W}}_3^T\hat{W}_3 - \frac{1}{\gamma_4}\dot{\hat{W}}_4^T\hat{W}_4 \qquad (59)\\ &\dot{H}(I_b, I_{FC}, I_{UC}, V_0)\\ &= z_1\left(\frac{V_{FC}}{L_{FC}} - \frac{R_{FC}}{L_{FC}}I_{FC} - \frac{(1-u_1)}{L_{FC}}V_0 + \dot{T}_1 - \dot{I}_{FC}^*\right)\\ &\quad + z_2\left(\frac{E_b}{L_b} - \frac{R_b}{L_b}I_b - \frac{u_2}{L_b}V_0 + \dot{T}_2 - \dot{I}_b^*\right)\\ &\quad + z_3\left(\frac{V_{UC}}{L_{UC}} - \frac{R_{UC}}{L_{UC}}I_{UC} - \frac{u_3}{L_{UC}}V_0 + \dot{T}_3 - \dot{I}_{UC}^*\right)\\ &\quad + z_4\left(\frac{(1-u_1)}{C_0}I_{FC} + \frac{D_{12}}{C_0}I_b\right.\\ &\quad \left.+\frac{D_{34}}{C_0}I_{UC} - \frac{1}{C_0}I_L + \dot{T}_4 - u_4\right) \qquad (60)\end{aligned}$$

Design PB-SMC for system (60) as follows:

$$u_1 = -\frac{L_{FC}}{V_0}\left(\frac{V_{FC}}{L_{FC}} - \frac{R_{FC}}{L_{FC}}I_{FC} - \frac{1}{L_{FC}}V_0 - \dot{I}_{FC}^* + \upsilon_1\right) \quad (61)$$

$$u_2 = \frac{L_b}{V_0}\left(\frac{E_b}{L_b} - \frac{R_b}{L_b}I_b - \dot{I}_b^* + \upsilon_2\right) \quad (62)$$

$$u_3 = \frac{L_{UC}}{V_0}\left(\frac{V_{UC}}{L_{UC}} - \frac{R_{UC}}{L_{UC}}I_{UC} - \dot{I}_{UC}^* + \upsilon_3\right) \quad (63)$$

$$u_4 = \left(\frac{(1-u_1)}{C_0}I_{FC} + \frac{u_2}{C_0}I_b + \frac{u_3}{C_0}I_{UC} - \frac{1}{C_0}I_L + \upsilon_4\right) \quad (64)$$

where υ_1, υ_2, υ_3, and υ_4 are auxiliary inputs which will be designed later. Inserting (61)-(64) into the derivative of storage function (60), yields:

$$\begin{aligned}&\dot{H}(I_b, I_{FC}, I_{UC}, V_0)\\ &= (I_{FC} - I_{FC}^*)\upsilon_1 + (I_b - I_b^*)\upsilon_2 + (I_{UC} - I_{UC}^*)\upsilon_3\\ &\quad + (V_0 - V_0^*)\upsilon_4 \qquad (65)\end{aligned}$$

The fractional-order PD^γ sliding mode surfaces are designed as follows:

$$\zeta_1 = D^\gamma(I_{FC} - I_{FC}^*) + \kappa_1(I_{FC} - I_{FC}^*) \quad (66)$$

$$\zeta_2 = D^\gamma(I_b - I_b^*) + \kappa_2(I_b - I_b^*) \quad (67)$$

$$\zeta_3 = D^\gamma(I_{UC} - I_{UC}^*) + \kappa_3(I_{UC} - I_{UC}^*) \quad (68)$$

$$\zeta_4 = D^\gamma(V_0 - V_0^*) + \kappa_4(V_0 - V_0^*) \quad (69)$$

where κ_i $i = 1, 2, 3, 4$ are positive constants. The attractiveness of the surfaces (66)-(69) ensures I_b, I_{FC}, I_{UC},

TABLE 3. Controller gains of the FCHEV system.

Parameters	Minimum
Battery module	288 v/13.9 Ah
PEMFC	350 V/250 A/34 kw
UC module	205 V/2700 F
C_0	1.66 mF
l_B, l_{FC}, and l_{UC}	3.30 mH
R_B, R_{FC}, and R_{UC}	20.0 $m\Omega$
Switching frequency	100 KHz
A	1.8 m^2
C_r	0.0048
C_x	0.19
g	9.81 N/kg
M	1066 kg
ρ_a	1.223 kg/m^3

and V_0 can effectively converge to their references. The auxiliary inputs are then established as follows:

$$\upsilon_1 = -\underbrace{\alpha_1(I_{FC} - I_{FC}^*)}_{\text{energy shaping}} - \underbrace{\lambda_1\zeta_1 - \rho_1 tanh(\zeta_1)}_{\text{robust terms}} \tag{70}$$

$$\upsilon_2 = -\underbrace{\alpha_2(I_b - I_b^*)}_{\text{energy shaping}} - \underbrace{\lambda_2\zeta_2 - \rho_2 tanh(\zeta_2)}_{\text{robust terms}} \tag{71}$$

$$\upsilon_3 = -\underbrace{\alpha_3(I_{UC} - I_{UC}^*)}_{\text{energy shaping}} - \underbrace{\lambda_3\zeta_3 - \rho_3 tanh(\zeta_3)}_{\text{robust terms}} \tag{72}$$

$$\upsilon_4 = -\underbrace{\alpha_4(V_0 - V_0^*)}_{\text{energy shaping}} - \underbrace{\lambda_4\zeta_4 - \rho_4 tanh(\zeta_4)}_{\text{robust terms}} \tag{73}$$

where α_i $i = 1, 2, 3, 4$ and λ_i $i = 1, 2, 3, 4$ are positive constants. Substituting (70)-(73) into (65) gives:

$$\begin{aligned}\dot{H}(I_b, I_{FC}, I_{UC}, V_0) \leq & -\alpha_1|z_1|^2 - \alpha_2|z_2|^2 \\ & - \alpha_3|z_3|^2 - \alpha_4|z_4|^2 - \bar{\alpha}_1|z_1| - \bar{\alpha}_2|z_2| \\ & - \bar{\alpha}_3|z_3| - \bar{\alpha}_4|z_4|\end{aligned} \tag{74}$$

where $|\lambda_1\zeta_1 + \rho_1 tanh(\zeta_1)| \leq \bar{\alpha}_1$, $|\lambda_2\zeta_2 + \rho_2 tanh(\zeta_2)| \leq \bar{\alpha}_2$, $|\lambda_3\zeta_3 + \rho_3 tanh(\zeta_3)| \leq \bar{\alpha}_3$, and $|\lambda_4\zeta_4 + \rho_4 tanh(\zeta_4)| \leq \bar{\alpha}_4$.

V. SIMULATION RESULTS

To check how accurate and useful the controllers shown in (61)-(64) were, a set of simulations were run on a 64-bit PC with an Intel(R) Core(TM) i7-10510U CPU running at 1.8GHz and 8GB of RAM using the MATLAB/Simulink software. For simulations, the sample size was set to 0.001s to find a good balance between computational resources and statistical significance. The ODE45 solver in Simulink was used to deal with the dynamic system equations that are part of our FCHEV control model while keeping the numbers stable. The performance of the proposed controllers was rigorously evaluated through a comparative analysis against alternative control methodologies, specifically the backstepping technique [27] and the variable structure control approach [31].

TABLE 4. Parameters and ratings of the FCHEV system.

Controller gains	Values
γ	0.5
κ_1, κ_2, κ_3, and κ_4	3, 3, 2, and 4
α_1, α_2, α_3, and α_4	6, 5, 4, and 7
λ_1, λ_2, λ_3, and λ_4	4, 4, 3, and 5
ρ_1, ρ_2, ρ_3, and ρ_4	2, 2, 2, and 3

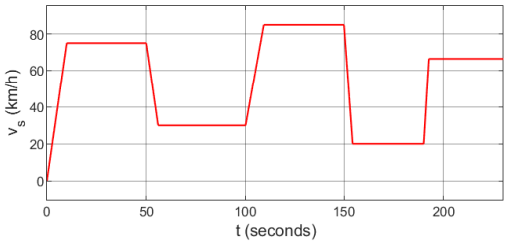

FIGURE 7. Vehicle speed profile.

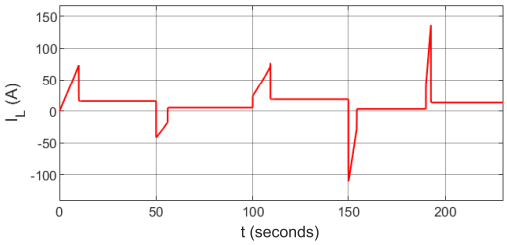

FIGURE 8. Load current requirement for different FCHEV speed.

The technical specifications of the FCHEV system under examination are comprehensively outlined in Table 3, providing the requisite context for the study. Additionally, Table 4 documents the precise gains that the controllers used for the sake of transparency. These rigorous assessments collectively contribute to the validation and verification of the efficacy and reliability of the proposed control strategies. The behavior and efficacy of passivity-based nonlinear control systems depend on parameters. Denoted by 'κ', γ, ρ, λ and 'α,' these variables are essential for optimizing control designs and ensuring desired attributes. For instance, control gains, which are positive constants, indicate the controller's potency and influence over the system, and we may adjust them to satisfy performance objectives. Control input limitations with positive constants also prevent excessive control attempts during practical implementations. Positive constants can also control convergence rates, affecting how quickly a system reaches equilibrium and careful selection is needed to provide the desired balance of stability, performance, and resilience while accounting for the controlled system's dynamics and restrictions.

As illustrated in Figure 7 is the driving cycle pattern characterizing the FCHEV's behavior, encompassing phases of acceleration, consistent velocity, and deceleration. This dynamic profile extends over a duration of 230 seconds, effectively spanning a distance of 8.31 kilometers.

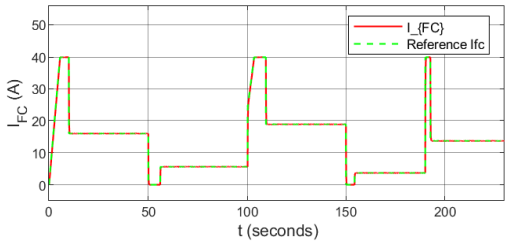

FIGURE 9. Fuel cell current supplied to the load.

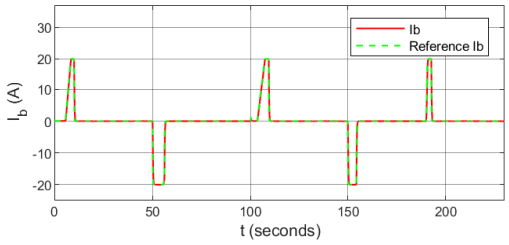

FIGURE 10. Battery current during the process of charging and discharging.

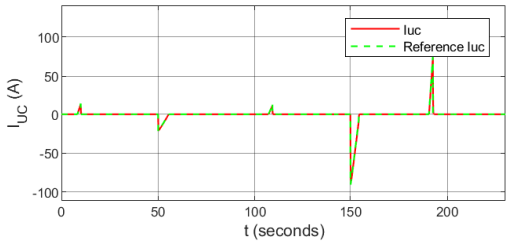

FIGURE 11. Ultra-capacitor current during charging and discharging modes to take care of the peak currents.

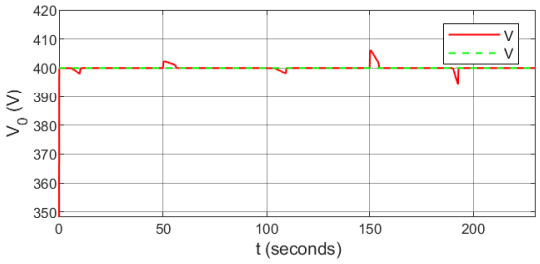

FIGURE 12. DC-bus voltage of the FCHEV during the driving cycle.

The corresponding load current requisites dictated by various speeds of the FCHEV are depicted in Figure 8. The simulation outcomes, attained while subjecting the FCHEV system to the control strategy proposed within this study, are presented in Figures 9 to 18. These graphical representations collectively serve to demonstrate the system's performance and behavior under the influence of the introduced controller. PBC stands out as an efficient control method in the fields of control engineering and robotics, with distinct advantages over other prevalent techniques. In contrast to PID control, which relies on error correction and can struggle with complex, nonlinear systems, PBC employs the principle of passivity to ensure system stability and resiliency in the face of a variety of disturbances. In contrast to model predictive control (MPC), which requires precision system models and computational resources, PBC excels in situations where accurate modeling is unavailable or insufficient [52]. It also contrasts favorably with sliding mode control (SMC), which, despite being robust, can result in undesirable chattering and sensitivity to parameter changes. PBC's primary strength is its ability to ensure energy dissipation within a system, making it ideally adapted for energy-sensitive applications, such as autonomous manipulators and mechanical systems [53]. In addition, PBC's ability to manage nonlinear systems without linearization or simplification, its inherent robustness, global asymptotic stability guarantees, and intuitive physical interpretation establish it as a potent control system design tool [54]. However, the choice of control method ultimately depends on the specific requirements and characteristics of the system, with PBC performing exceptionally well when dealing with complex, uncertain, and nonlinear systems.

Figure 9 presents the trajectory curves of the FC-supplied current to the load. In instances where the current demand remains optimal ($I_{FC} < 40\ A$), the FC is supplying current only to the load. Furthermore, during high load demand ($I_{FC} > 40\ A$) and deceleration, the FC is also supplying the current to prevent degradation. Similarly, Figure 10 delineates the course of the battery-supplied current. The battery discharges and furnishes current during periods marked by elevated load demands and instances of acceleration, functioning as a compensatory measure for the FC. Furthermore, during deceleration stages, the battery regains current to recharge itself. To ensure the longevity of the battery, a current limiter is integrated, maintaining the battery current within the range of $(-20 \leq I_b^* \leq 20\ A)$. This precautionary measure is taken to extend the operational lifespan of the battery.

Additionally, the representation of the UC current's behavior can be observed in Figure 11. In situations of elevated load demand, both the battery and FC experience limitations in delivering the required peak load current due to their constrained power densities. To address this, the UC discharges, effectively assuming the role of compensating for peak load current demand. This discharge action not only alleviates potential strain on the battery and FC but also helps maintain their optimal functionality. Similarly, during regenerative braking phases, the UC recharges by recuperating the peak negative current, thereby playing a dual role in both energy recovery and alleviating stress on the battery. Finally, Figure 12 provides insight into the trajectory of the DC-bus voltage. This voltage exhibits fluctuations ranging between $394V$ and $406V$ when the vehicle experiences acceleration or deceleration. The proposed controller intervenes during these voltage fluctuations, aiming to restore the voltage to its reference value. This active voltage regulation serves to ensure stable system performance, effectively mitigating any potential deviations from the desired operational parameters.

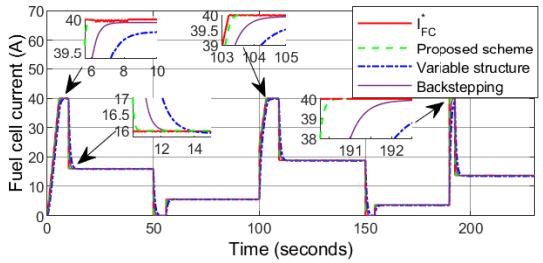

FIGURE 13. Fuel cell current curves under three control techniques.

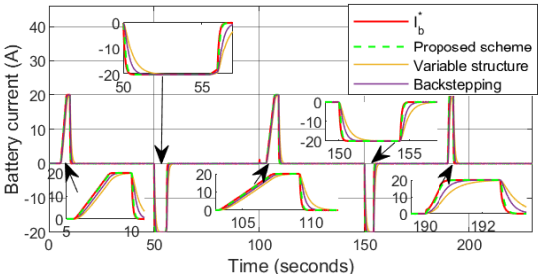

FIGURE 14. Battery current curves under three control techniques.

Because of this, the experimental results show that the variables I_{FC}, I_b, I_{UC}, and V_0 always stay in sync with their corresponding reference values, even when the load changes. The aforementioned pattern is prominently exhibited in Figures 7 through 12. The results of this study provide strong evidence for the effectiveness of the controller that was designed. The findings demonstrate that each energy storage component effectively performs its intended function in response to the demands placed on it, in accordance with their specific technological capabilities as outlined in the energy management framework.

The Figures illustrate the comparative outcomes of the suggested control system, backstepping, variable structure control approaches, and control signal as shown in Figures 13-18 and Figure 19, respectively. The tracking results of the three control approaches exhibit a pretty high level of performance. To further illustrate the practicality of proposed scheme and its impact of storage component SOC on FCHEVs, various SOC values are implemented. The findings for the batteries cells 30% SOC (Scenario A) are depicted in Figure 15, where Figure 16 represents the batteries cells 50% SOC (Scenario B). In the given circumstance, the batteries pack current accurately adheres to the baseline (the reference current) value during the state of stability as shown in left side of Figure 15. Nevertheless, instances of overshoot are detected throughout the initial phase, transitional stages, and in the condition of fault event. The occurrence of overshoots can be observed at two specific time instances, namely $t = 5s$ and $t = 25s$, in the fault example as shown in right side of Figure 15. During these instances, the battery current reaches an estimated level of 0.5 A. The illustration on the opposite side demonstrates the influence of a 30% SOC on the baseline current of the cell. In Scenario B, the battery cells pack SOC is set to 50% as depicted in left side of Figure 16. Similar observations are noted in contrast to the after-mentioned results, although the specific values of both the battery current and its baseline in the fault example as shown in left side of Figure 16. The battery current in this specific scenario is roughly 0.8 amperes. Under these circumstances, the SOC reduces by two percent in terms of percentage value. These results shows the supremacy of proposed approach considering the fault scenarios. In contrast to the other two ways, the suggested control strategy effectively addresses variations in load demand by promptly and correctly supplying the necessary currents and stabilizing the DC-bus voltage. It outperforms the alternative methods in terms of mitigating overshooting, undershooting, and deviations in the DC bus voltage.

VI. RESULTS IMPLICATIONS AND SUMMARY

This research could benefit FCHEVs and renewable energy. The optimized FCHEV energy management improves vehicle performance and efficiency, making FCHEVs more appealing. As they become more widespread, FCHEVs cut greenhouse gas emissions and air pollution, making transportation greener. Range anxiety among potential FCHEV purchasers can be alleviated by the study's focus on vehicle range. Optimizing the energy management system eliminates this issue and makes FCHEVs more appealing to consumers by extending their hydrogen tank range. Importantly, this innovation improved fuel cell durability. Consumers and commercial fleet operators benefit from cheaper FCHEV maintenance costs and longer lifespans.

FCHEVs and sustainable transportation energy integration benefit from the research. Hydrogen fuel cell FCHEVs combine renewable energy and transportation. Solar and wind power can be more seamlessly integrated into hydrogen fuel manufacturing thanks to the study. This synergy reduces fossil fuel use and promotes sustainable energy and climate change. The study's greenhouse gas emission reductions and fuel efficiency increases demonstrate its environmental impact. FCHEVs with optimized energy management systems can significantly reduce carbon emissions and support global climate goals. The study can inform policymakers about FCHEVs' benefits. To promote FCHEV usage and sustainable energy, this data can inform tax incentives, rebates, and hydrogen refueling infrastructure. Finally, the study's recommendations for renewable energy integration research aid researchers and developers. It encourages FCHEV innovation for sustainable energy and ongoing improvement. This study will improve vehicle performance, reduce environmental impact, and develop renewable energy initiatives, making it vital to clean and sustainable transportation. Table 5 present a performance comparison of the proposed controllers in tracking I^*_{Fc}. The results demonstrate that the proposed scheme achieves lower settling time and root mean square (RMS) error values compared to other advanced methods, including variable structure and backstepping approaches. Tables 6 and 7 display the performance

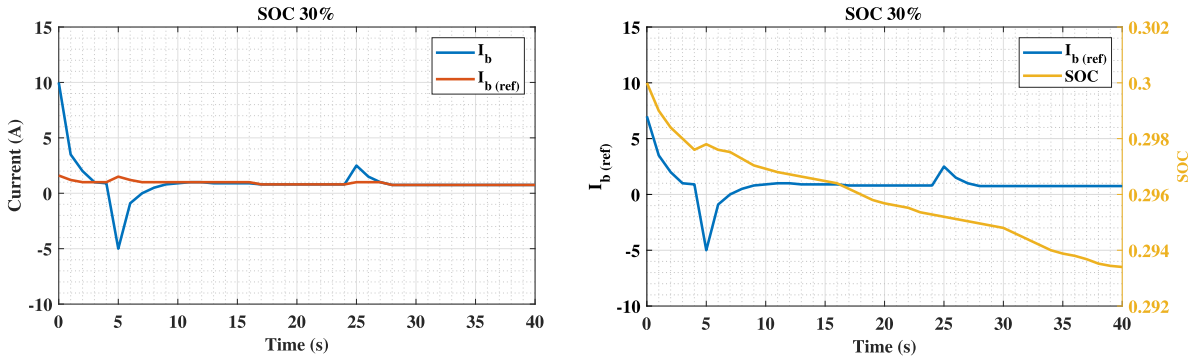

FIGURE 15. Fault events for 30% SOC (Scenario A).

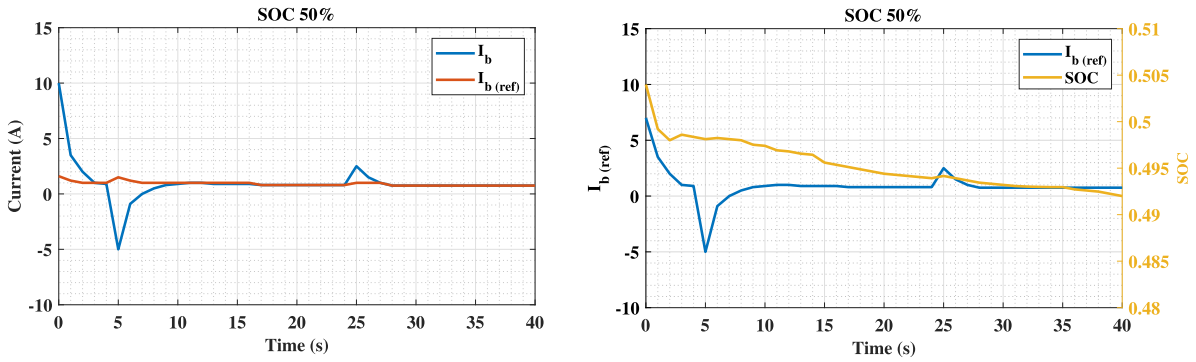

FIGURE 16. Fault events for 50% SOC (Scenario B).

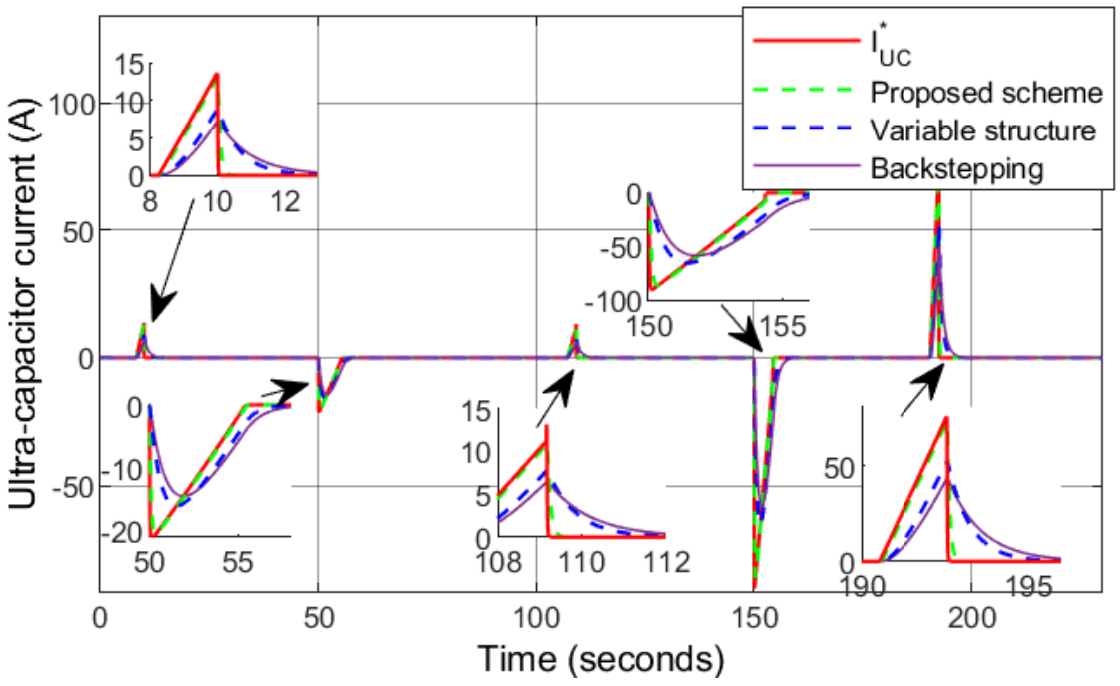

FIGURE 17. Ultra-capacitor current under three control techniques.

comparison of the proposed controllers for tracking I_b^*, and I_{UC}^*, respectively. Once again, the results clearly indicate that the proposed approaches outperform other advanced control methods, exhibiting lower RMS values and settling times in comparison to variable structure and backstepping control approaches. The efficacy of the proposed method can also be

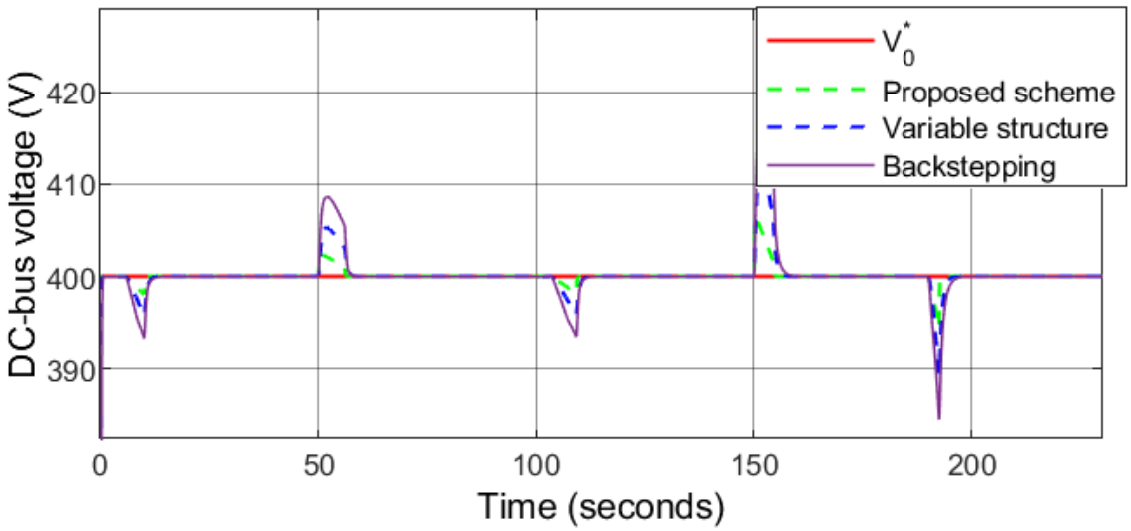

FIGURE 18. DC-bus voltage under three control techniques.

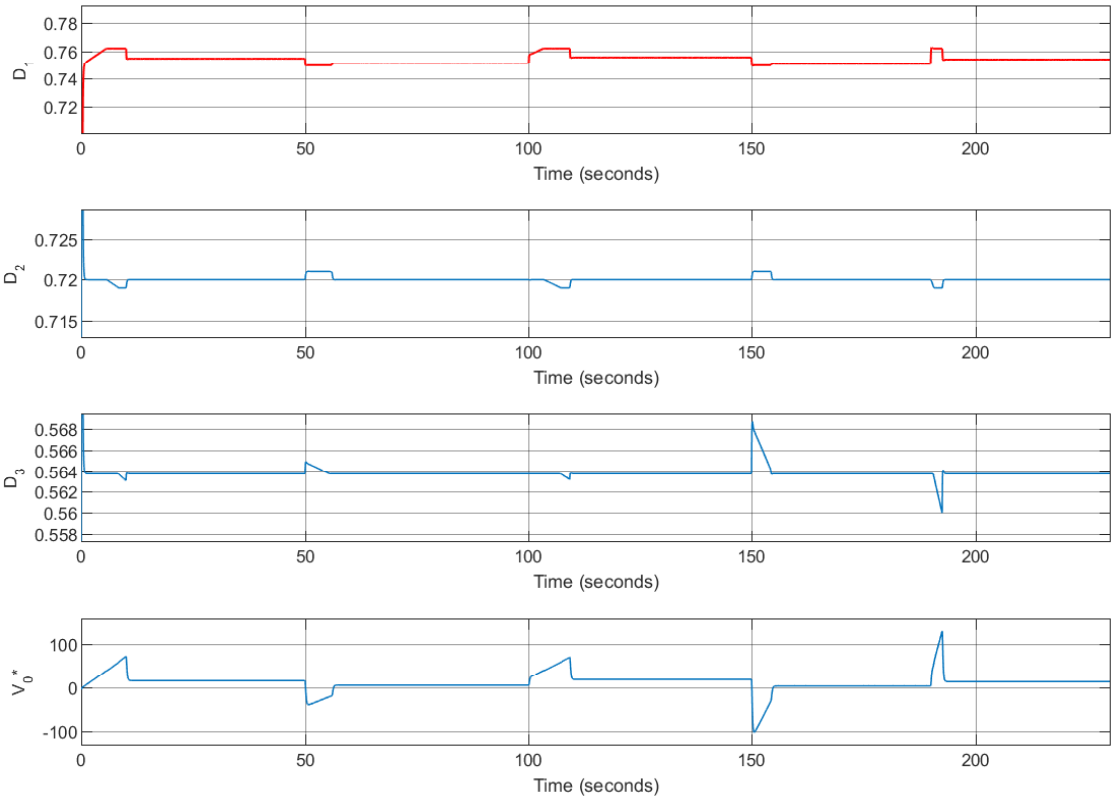

FIGURE 19. Control signals.

further seen for performance comparison of the controllers for tracking V_0^* presented in Table 8. The suggested scheme once again attain lower time of stabilization and RMS value. The results further showcases that the proposed scheme is more rigours and practical as compared with other advanced approaches.

VII. PERSPECTIVE TRENDS FOR FCHEV

The future trajectory of FCHEVs is characterized by a multitude of promising trends and prospective avenues. An observable phenomenon in the field of energy planning and management is the increasing incorporation of machine learning and artificial intelligence [55]. The implementation

TABLE 5. Performance comparison of the controllers for tracking I_{Fc}^{*}.

Controller	Settling time	RMS of errors
Proposed scheme	0.7023 s	1.288
Variable structure control	2.781 s	2.902
Backstepping control	2.424 s	2.175

TABLE 6. Performance comparison of the controllers for tracking I_{b}^{*}.

Controller	Settling time	RMS of errors
Proposed scheme	0.7350 s	0.4244
Variable structure control	2.320 s	1.839
Backstepping control	2.159 s	1.234

TABLE 7. Performance comparison of the controllers for tracking I_{UC}^{*}.

Controller	Settling time	RMS of errors
Proposed scheme	0.9020 s	2.516
Variable structure control	2.341 s	5.109
Backstepping control	3.014 s	5.807

TABLE 8. Performance comparison of the controllers for tracking V_{0}^{*}.

Controller	Settling time	RMS of errors
Proposed scheme	0.4020 s	18.530
Variable structure control	1.093 s	19.990
Backstepping control	1.793 s	21.370

of this integration has the potential to enhance the capabilities of vehicles by enabling them to acquire knowledge and anticipate the most effective control techniques by analyzing current driving situations. As a result, there is a possibility of achieving substantial advancements in energy efficiency. Another area of research that shows great potential is the advancement of cyber-physical systems, which involve the seamless integration of computer and physical elements [56]. The use of this methodology has the potential to improve the exchange of information across different vehicle elements, leading to enhanced accuracy in regulation and synchronization, hence increasing the overall energy efficiency in FCHEVs. The utilization of predictive analytics and sophisticated computing approaches is likewise a noteworthy trend [57]. The utilization of predictive control and optimization models has the potential to enhance the precision of power demand forecasting, thereby facilitating more effective real-time energy allocation. Predictive algorithms have the potential to optimize energy distribution and charging procedures, thereby augmenting the efficiency of EVs. Furthermore, the field of FC technology is experiencing significant progress, characterized by the emergence of enhanced, durable, and economically viable FC systems. It is anticipated that scholars would investigate the potential integration of these breakthroughs into energy management systems, which may have a transformative impact on the area [58]. Additionally, it is anticipated that the advent of autonomous vehicles and vehicle-to-vehicle communication would give rise to collaborative energy management solutions. Vehicles have the potential to exchange data pertaining to their routes and energy requirements, hence facilitating collaborative optimization for enhanced energy efficiency within a network of vehicles [59].

VIII. CONCLUSION

This study introduces a new passivity-based control framework that is designed to make the best use of power allocation and energy management in hybrid energy storage systems. It is especially made to meet the needs of FCHEVs. The meticulously devised control system incorporates a fault-tolerant strategy integrated with an energy management system, considering the complex dynamics of the battery, FC, and UC. The implementation utilises power converters connecting energy sources to the vehicle's DC bus. To demonstrate the effectiveness of our control architecture, we employed the MATLAB/Simulink software platform. The proposed controller plays a crucial role in overseeing and regulating reference currents for hybrid energy storage systems, following a predefined current sharing protocol. This ensures the FCHEV can efficiently meet power demands across various driving conditions. The suggested passivity-based nonlinear control system improves settling time and RMS voltage by a lot, performing better than both variable structure control and backstepping control. Furthermore, the study enhances its originality by taking into account sensor and SOC faults. When dealing with SOC failures, adding additional control input improves the performance of the controller, making the convergence faster and enhancing the robustness of the closed-loop FCHEV system. Moreover, our control architecture excels at precisely managing the DC-bus voltage, maintaining stability even in dynamic driving situations and when encountering faults in FCHEVs and batteries. Going forward, our aim is to delve deeper into the resilience and reliability of our proposed model by applying the Lyapunov stability criterion. Additionally, we will assess the robustness of the model against parameter variations and system uncertainties, incorporating driver behaviour profiles into state space models. Comprehensively examining DC-bus fault mitigation in FCHEVs will be the main focus of further research, which will then include experimental validation.

REFERENCES

[1] Z. Zhu, Y. Zhang, Z. Deng, and M. Wang, "A novel voltage sag detection method for analyzing charging quality of electric vehicle," *Comput. Electr. Eng.*, vol. 112, Dec. 2023, Art. no. 108991.
[2] O. Oloruntobi, K. Mokhtar, A. Gohari, S. Asif, and L. F. Chuah, "Sustainable transition towards greener and cleaner seaborne shipping industry: Challenges and opportunities," *Cleaner Eng. Technol.*, vol. 13, Apr. 2023, Art. no. 100628.
[3] Q. Wang, C. Sun, and Y. Gu, "Research on SOC estimation method of hybrid electric vehicles battery based on the grey wolf optimized particle filter," *Comput. Electr. Eng.*, vol. 110, Sep. 2023, Art. no. 108907.
[4] I. Ahmed, M. Rehan, K.-S. Hong, and A. Basit, "A consensus-based approach for economic dispatch considering multiple fueling strategy of electricity production sector over a smart grid," in *Proc. 13th Asian Control Conf.*, 2022, pp. 1196–1201.

[5] I. Ahmed, M. Rehan, A. Basit, and K.-S. Hong, "Greenhouse gases emission reduction for electric power generation sector by efficient dispatching of thermal plants integrated with renewable systems," *Sci. Rep.*, vol. 12, no. 1, p. 12380, Jul. 2022.

[6] K. A. Khan, M. M. Quamar, F. H. Al-Qahtani, M. Asif, M. Alqahtani, and M. Khalid, "Smart grid infrastructure and renewable energy deployment: A conceptual review of Saudi Arabia," *Energy Strategy Rev.*, vol. 50, Nov. 2023, Art. no. 101247.

[7] U. Akram, M. Khalid, and S. Shafiq, "An innovative hybrid wind-solar and battery-supercapacitor microgrid system—Development and optimization," *IEEE Access*, vol. 5, pp. 25897–25912, 2017.

[8] I. Ahmed, A. Irshad, S. Zafar, B. A. Khan, M. Raza, and P. R. Ali, "The role of environmental initiatives and green value co-creation as mediators: Promoting corporate entrepreneurship and green innovation," *Social Netw. Bus. Econ.*, vol. 3, no. 4, p. 85, Mar. 2023.

[9] S. Aziz, I. Ahmed, K. Khan, and M. Khalid, "Emerging trends and approaches for designing net-zero low-carbon integrated energy networks: A review of current practices," *Arabian J. Sci. Eng.*, vol. 49, no. 5, pp. 6163–6185, May 2024.

[10] T. B. Nadeem, M. Siddiqui, M. Khalid, and M. Asif, "Distributed energy systems: A review of classification, technologies, applications, and policies," *Energy Strategy Rev.*, vol. 48, Jul. 2023, Art. no. 101096.

[11] U.-E.-H. Alvi, I. Ahmed, S. R. Hasan, B. Ashfaq, M. Raza, and S. Mukhtar, "Adaptive swarm intelligence-based optimization approach for smart grids power dispatch," in *Proc. Int. Conf. Emerg. Technol. Electron., Comput. Commun.*, 2022, pp. 1–6.

[12] S. Alshahrani, M. Khalid, and M. Almuhaini, "Electric vehicles beyond energy storage and modern power networks: Challenges and applications," *IEEE Access*, vol. 7, pp. 99031–99064, 2019.

[13] I. Ahmed, M. Rehan, A. Basit, M. Tufail, and K.-S. Hong, "Neuro-fuzzy and networks-based data driven model for multi-charging scenarios of plug-in-electric vehicles," *IEEE Access*, vol. 11, pp. 87150–87165, 2023.

[14] I. Ahmed, M. Rehan, A. Basit, M. Tufail, and K.-S. Hong, "A dynamic optimal scheduling strategy for multi-charging scenarios of plug-in-electric vehicles over a smart grid," *IEEE Access*, vol. 11, pp. 28992–29008, 2023.

[15] F. Ali, I. Ahmed, and W. Sarwar, "Modeling and simulation of vehicles's energy conversion techniques," *Power Generation System Renewable Energy Technologies*, pp. 1–5, 2015.

[16] A. Seitaridis, E. S. Rigas, N. Bassiliades, and S. D. Ramchurn, "An agent-based negotiation scheme for the distribution of electric vehicles across a set of charging stations," *Simul. Model. Pract. Theory*, vol. 100, Apr. 2020, Art. no. 102040.

[17] M. Maaruf and M. Khalid, "Power quality control of hybrid wind/electrolyzer/fuel-cell/bess microgrid," *IEEE PES Innov. Smart Grid Technol.-Asia*, pp. 1–5, Dec. 2021.

[18] B. Yang, J. Wang, Y. Sang, L. Yu, H. Shu, S. Li, T. He, L. Yang, X. Zhang, and T. Yu, "Applications of supercapacitor energy storage systems in microgrid with distributed generators via passive fractional-order sliding-mode control," *Energy*, vol. 187, Nov. 2019, Art. no. 115905.

[19] B. Yang, L. Jiang, W. Yao, and Q. H. Wu, "Perturbation estimation based coordinated adaptive passive control for multimachine power systems," *Control Eng. Pract.*, vol. 44, pp. 172–192, Nov. 2015.

[20] Y. Bo, W. Junting, Y. Lei, C. Pulin, S. Hongchun, and Y. Tao, "Peafowl optimization algorithm based bi-level multi-objective optimal allocation of energy storage systems in distribution network," *J. Shanghai Jiaotong Univ.*, vol. 56, no. 10, p. 1294, 2022.

[21] A. A. Panagopoulos, F. Christianos, M. Katsigiannis, K. Mykoniatis, G. Chalkiadakis, M. Pritoni, T. Peffer, O. P. Panagopoulos, E. S. Rigas, D. E. Culler, N. R. Jennings, and T. Lipman, "IPlugie: Intelligent electric vehicle charging in buildings with grid-connected intermittent energy resources," *Simul. Model. Pract. Theory*, vol. 115, Feb. 2022, Art. no. 102439.

[22] S. Sezen, E. Karakas, K. Yilmaz, and M. Ayaz, "Finite element modeling and control of a high-power SRM for hybrid electric vehicle," *Simul. Model. Pract. Theory*, vol. 62, pp. 49–67, Mar. 2016.

[23] M. M. Islam, S. A. Siffat, I. Ahmad, M. Liaquat, and S. A. Khan, "Adaptive nonlinear control of unified model of fuel cell, battery, ultracapacitor and induction motor based hybrid electric vehicles," *IEEE Access*, vol. 9, pp. 57486–57509, 2021.

[24] A. Demircalı, P. Sergeant, S. Koroglu, S. Kesler, E. Öztürk, and M. Tumbek, "Influence of the temperature on energy management in battery-ultracapacitor electric vehicles," *J. Cleaner Prod.*, vol. 176, pp. 716–725, Mar. 2018.

[25] H. Jiang, L. Xu, J. Li, Z. Hu, and M. Ouyang, "Energy management and component sizing for a fuel cell/battery/supercapacitor hybrid powertrain based on two-dimensional optimization algorithms," *Energy*, vol. 177, pp. 386–396, Jun. 2019.

[26] H. Armghan, I. Ahmad, N. Ali, M. F. Munir, S. Khan, and A. Armghan, "Nonlinear controller analysis of fuel cell–battery–ultracapacitor-based hybrid energy storage systems in electric vehicles," *Arabian J. Sci. Eng.*, vol. 43, no. 6, pp. 3123–3133, Jun. 2018.

[27] M. F. Munir, I. Ahmad, S. A. Siffat, M. A. Qureshi, H. Armghan, and N. Ali, "Non-linear control for electric power stage of fuel cell vehicles," *ISA Trans.*, vol. 102, pp. 117–134, Jul. 2020.

[28] Z. Fu, Z. Li, P. Si, and F. Tao, "A hierarchical energy management strategy for fuel cell/battery/supercapacitor hybrid electric vehicles," *Int. J. Hydrogen Energy*, vol. 44, no. 39, pp. 22146–22159, Aug. 2019.

[29] H. Fathabadi, "Novel fuel cell/battery/supercapacitor hybrid power source for fuel cell hybrid electric vehicles," *Energy*, vol. 143, pp. 467–477, Jan. 2018.

[30] S. Qiu, L. Qiu, L. Qian, and P. Pisu, "Hierarchical energy management control strategies for connected hybrid electric vehicles considering efficiencies feedback," *Simul. Model. Pract. Theory*, vol. 90, pp. 1–15, Jan. 2019.

[31] A. U. Rahman, I. Ahmad, and A. S. Malik, "Variable structure-based control of fuel cell-supercapacitor-battery based hybrid electric vehicle," *J. Energy Storage*, vol. 29, Jun. 2020, Art. no. 101365.

[32] F. Tao, L. Zhu, Z. Fu, P. Si, and L. Sun, "Frequency decoupling-based energy management strategy for fuel cell/battery/ultracapacitor hybrid vehicle using fuzzy control method," *IEEE Access*, vol. 8, pp. 166491–166502, 2020.

[33] J. Chen and Q. Song, "A decentralized dynamic load power allocation strategy for fuel cell/supercapacitor-based APU of large more electric vehicles," *IEEE Trans. Ind. Electron.*, vol. 66, no. 2, pp. 865–875, Feb. 2019.

[34] V. V. Joshi, N. Mishra, and D. Malviya, "A vector control based supercapacitor current control algorithm for fuel cell and battery—Supercapacitor integrated electric vehicles," in *Proc. IEEE 8th Power India Int. Conf.*, Dec. 2018, pp. 1–6.

[35] R. Ortega, A. van der Schaft, F. Castanos, and A. Astolfi, "Control by interconnection and standard passivity-based control of port-Hamiltonian systems," *IEEE Trans. Autom. Control*, vol. 53, no. 11, pp. 2527–2542, Dec. 2008.

[36] W. Gil-González, O. D. Montoya, and A. Garces, "Standard passivity-based control for multi-hydro-turbine governing systems with surge tank," *Appl. Math. Model.*, vol. 79, pp. 1–17, Mar. 2020.

[37] C. D. García-Beltrán, E. M. Miranda-Araujo, M. E. Guerrero-Sanchez, G. Valencia-Palomo, O. Hernández-González, and S. Gómez-Peñate, "Passivity-based control laws for an unmanned powered parachute aircraft," *Asian J. Control*, vol. 23, no. 5, pp. 2087–2096, Sep. 2021.

[38] G. L. Magaldi, F. M. Serra, C. H. de Angelo, O. D. Montoya, and D. A. Giral-Ramírez, "Voltage regulation of an isolated DC microgrid with a constant power load: A passivity-based control design," *Electronics*, vol. 10, no. 17, p. 2085, Aug. 2021.

[39] B. Yang, T. Yu, H. Shu, Y. Zhang, J. Chen, Y. Sang, and L. Jiang, "Passivity-based sliding-mode control design for optimal power extraction of a PMSG based variable speed wind turbine," *Renew. Energy*, vol. 119, pp. 577–589, Apr. 2018.

[40] Y. Ma, J. Chen, J. Wang, Y. Xu, and Y. Wang, "Path-tracking considering yaw stability with passivity-based control for autonomous vehicles," *IEEE Trans. Intell. Transp. Syst.*, vol. 23, no. 7, pp. 8736–8746, Jul. 2022.

[41] I.-S. Sorlei, N. Bizon, P. Thounthong, M. Varlam, E. Carcadea, M. Culcer, M. Iliescu, and M. Raceanu, "Fuel cell electric vehicles—A brief review of current topologies and energy management strategies," *Energies*, vol. 14, no. 1, p. 252, Jan. 2021.

[42] S. J. Moura, H. K. Fathy, D. S. Callaway, and J. L. Stein, "A stochastic optimal control approach for power management in plug-in hybrid electric vehicles," *IEEE Trans. Control Syst. Technol.*, vol. 19, no. 3, pp. 545–555, May 2011.

[43] H. S. Das, C. W. Tan, and A. H. M. Yatim, "Fuel cell hybrid electric vehicles: A review on power conditioning units and topologies," *Renew. Sustain. Energy Rev.*, vol. 76, pp. 268–291, Sep. 2017.

[44] M. A. Hassan, C.-L. Su, J. Pou, G. Sulligoi, D. Almakhles, D. Bosich, and J. M. Guerrero, "DC shipboard microgrids with constant power loads: A review of advanced nonlinear control strategies and stabilization techniques," *IEEE Trans. Smart Grid*, vol. 13, no. 5, pp. 3422–3438, Sep. 2022.
[45] A. Nduwamungu, T. T. Lie, I. Lestas, N.-K.-C. Nair, and K. Gunawardane, "Control strategies and stabilization techniques for DC/DC converters application in DC MGs: Challenges, opportunities, and prospects—A review," *Energies*, vol. 17, no. 3, p. 669, Jan. 2024.
[46] M. Maaruf and M. Khalid, "Global sliding-mode control with fractional-order terms for the robust optimal operation of a hybrid renewable microgrid with battery energy storage," *Electronics*, vol. 11, no. 1, p. 88, Dec. 2021.
[47] F. Castaños and R. Ortega, "Energy-balancing passivity-based control is equivalent to dissipation and output invariance," *Syst. Control Lett.*, vol. 58, no. 8, pp. 553–560, Aug. 2009.
[48] R. Ortega and I. Mareels, "Energy-balancing passivity-based control," in *Proc. Amer. Control Conf. ACC*, 2000, pp. 1265–1270.
[49] M. R. Naseh and A. Behdani, "Non-linear control of fuel cell/ultra-capacitor hybrid electric vehicle using comprehensive function algorithm based on IDA-PBC," *Adv. Energy Convers. Mater.*, vol. 1, pp. 1–17, Feb. 2023.
[50] M. Vasiladiotis, A. Rufer, and A. Béguin, "Modular converter architecture for medium voltage ultra fast EV charging stations: Global system considerations," in *Proc. IEEE Int. Electr. Vehicle Conf.*, Mar. 2012, pp. 1–7.
[51] Z. E. Huma, M. K. Azeem, I. Ahmad, H. Armghan, S. Ahmed, and H. M. M. Adil, "Robust integral backstepping controller for energy management in plugin hybrid electric vehicles," *J. Energy Storage*, vol. 42, Oct. 2021, Art. no. 103079.
[52] F. Kamal and B. Chowdhury, "Model predictive control and optimization of networked microgrids," *Int. J. Electr. Power Energy Syst.*, vol. 138, Jun. 2022, Art. no. 107804.
[53] J. George, G. Mani, and A. Alexander Stonier, "An extensive critique of sliding mode control and adaptive neuro-fuzzy inference system for nonlinear system," *Asian J. Control*, vol. 24, no. 5, pp. 2548–2564, Sep. 2022.
[54] S. Monesha and S. Ganesh Kumar, "Microgrid: Recent trends and control," *Power Converters, Drives Controls Sustain. Oper.*, pp. 595–629, 2023.
[55] X. Zhang, X. Kong, R. Yan, Y. Liu, P. Xia, X. Sun, R. Zeng, and H. Li, "Data-driven cooling, heating and electrical load prediction for building integrated with electric vehicles considering occupant travel behavior," *Energy*, vol. 264, Feb. 2023, Art. no. 126274.
[56] M. Hamzah, M. M. Islam, S. Hassan, M. N. Akhtar, M. J. Ferdous, M. B. Jasser, and A. W. Mohamed, "Distributed control of cyber physical system on various domains: A critical review," *Systems*, vol. 11, no. 4, p. 208, Apr. 2023.
[57] P. Patil, K. Kazemzadeh, and P. Bansal, "Integration of charging behavior into infrastructure planning and management of electric vehicles: A systematic review and framework," *Sustain. Cities Soc.*, vol. 88, Jan. 2023, Art. no. 104265.
[58] T. Hai, J. Zhou, and M. Khaki, "Optimal planning and design of integrated energy systems in a microgrid incorporating electric vehicles and fuel cell system," *J. Power Sources*, vol. 561, Mar. 2023, Art. no. 232694.
[59] X. Chen, S. Leng, J. He, L. Zhou, and H. Liu, "The upper bounds of cellular vehicle-to-vehicle communication latency for platoon-based autonomous driving," *IEEE Trans. Intell. Transp. Syst.*, vol. 24, no. 7, pp. 6874–6887, Jul. 2023.

MUHAMMAD KHALID (Senior Member, IEEE) received the Ph.D. degree in electrical engineering from the School of Electrical Engineering Telecommunications (EET), University of New South Wales (UNSW), Sydney, Australia, in 2011. He was a Postdoctoral Research Fellow for three years and then he continued as a Sr. Research Associate with the Australian Energy Research Institute, School of EET, UNSW, for another two years. He is currently an Associate Professor with the Electrical Engineering Department, King Fahd University of Petroleum Minerals (KFUPM), Dhahran, Saudi Arabia. He has authored/-coauthored several journal and conference papers in the field of control and optimization for renewable power systems. His current research interests include the optimization and control of battery energy storage systems for large-scale grid-connected renewable power plants (particularly wind and solar), distributed power generation and dispatch, hybrid energy storage, hydrogen systems, EVs, and smart grids. He was a recipient of a highly competitive post-doctoral writing fellowship from UNSW, in 2010. He was a recipient of many academic awards and research fellowships. He has been a reviewer for numerous international journals and conferences.